

Solvent Co-intercalation: An Emerging Mechanism in Li-, Na-, and K-Ion Capacitors

Madhusoodhanan Lathika Divya, Yun-Sung Lee, and Vanchiappan Aravindan*



Cite This: *ACS Energy Lett.* 2021, 6, 4228–4244



Read Online

ACCESS |



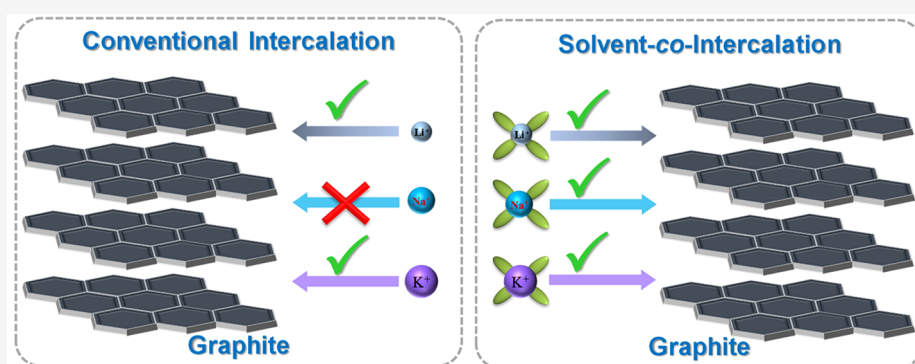
Metrics & More



Article Recommendations



Supporting Information



ABSTRACT: Solvated-ion intercalation or co-intercalation reactions make graphite a versatile anode for Na-ion chemistry and beyond. This alternate intercalation mechanism could overcome the difficulties faced by conventional intercalation reactions with graphite. The proper choice of the solvent molecule could co-intercalate Na-, Li-, and K-ions with high capacity and power density values, which are tailor-made for metal-ion capacitor (MIC, M = Li, Na, and K) applications. This review summarizes significant advances in co-intercalation chemistry, research progress in MICs with a graphite anode, and activated carbon cathodes in glyme family solutions. Also, we compare the advantages and challenges of MICs with the co-intercalation-based mechanism in place of conventional graphite anodes with bare-ion intercalation. The progress indicates high-performance hybrid-ion capacitors with high power capability and fast reaction kinetics. At the same time, it is essential to find methods to improve the energy-storage capability of such MICs to realize their commercial reality.

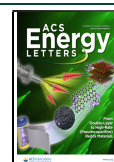
As the world grudgingly crosses the threshold of the second wave of the COVID-19 pandemic, we could observe a shift in global energy demand along with diverse patterns of energy consumption.^{1,2} Even though the overall energy demand declines, there is an increase in household energy consumption due to government measures against the spread of the corona virus.^{3,4} It is vital to ensure a secure, sustainable energy future to raise the standard of living and also to fulfill the financial development plans for the economic growth of countries such as India.^{5,6} Today, renewable energy covers more than 30% of our energy requirement. Growing solar and wind technology deployment is crucial to edge out fossil fuels and tumble greenhouse gas emissions. However, these technologies have intermittent output and, hence, entail efficient electrical energy-storage systems (EESs) to flatten the electricity supply from these sources and guarantee that supply matches demand.⁷ Rechargeable batteries that use electrochemical oxidation–reduction reactions to translate the chemical energy of the active material into electrical energy are mainly utilized for

EESs. Lithium-ion batteries (LIBs) are usually considered for compact electronic devices and are rapidly entering the transportation sector. They can store more energy (150–200 Wh kg^{−1}), but they take hours to get recharged when they are drained out (power density <1 kW kg^{−1} and lifespan <10³ times). Supercapacitors or electrochemical capacitors (electric double-layer capacitors, EDLCs) are commonly used for rapid power delivery and recharging applications (power density >5 kW kg^{−1} and life span >10⁵ times); however, they have limited energy-storage capacity (<10 Wh kg^{−1}). Nevertheless, modern technologies necessitate a much more significant amount of energy stored with high power, swiftly and at a low cost.^{6,8,9}

Received: August 25, 2021

Accepted: October 28, 2021

Published: November 8, 2021



The most intuitive way to bring together high energy and power within a single device is to assemble a hybrid configuration of different energy-storage devices. Metal-ion hybrid capacitors (MICs), mainly lithium-ion capacitors (LICs), are hybrid EESs formed by merging the insertion/de-insertion mechanism of LIB electrodes with the adsorption/desorption mechanism of EDLC electrodes.^{10–13} Amatucci et al.¹⁴ introduced the first LIC in 2001 using a nanostructured $\text{Li}_4\text{Ti}_5\text{O}_{12}$ anode, an activated carbon (AC) cathode, and Li-ion-containing aprotic organic solutions (e.g., LiPF_6 in ethylene carbonate (EC):dimethyl carbonate) via a topotactic intercalation process. The LICs have advantages over LIBs (longer lifetime and high specific power) and EDLCs (higher working voltage and high specific energy). Hence, they have particular applications, such as un-interruptible power source systems, photovoltaic power generation, wind power generation systems, voltage sag compensation, electric and hybrid electric vehicle technology, and energy recovery systems such as regenerative braking. LICs, with two electrodes (battery and capacitive type) composed of carbonaceous materials (dual-carbon LICs), are the most inspiring type because of their low cost and stable performance compared to other configurations with metal-containing intercalation-type or alloy/conversion-type negative (battery) electrodes.^{15–18}

Moreover, LICs with AC cathodes and pre-lithiated graphitic anodes have been commercialized productively.¹⁹ However, rare and unevenly distributed lithium resources cause supply chain crunches to limit the growth of Li-based EESs. Research on MICs with Na^+ and K^+ in place of Li^+ is rising, considering aspects such as abundant Na/K resources and similarity in physicochemical properties. The first sodium-ion capacitor (NIC) was reported in 2012 by Chen et al.^{20,21} using V_2O_5 nanowires as anode with an AC cathode. In the meantime, due to increasing interest in potassium-ion batteries (KIBs), a potassium-ion capacitor (KIC) was also parallelly explored in 2017.²² Since then, the research interest in MICs has made significant progress in finding different electrode materials, including carbonaceous material-based electrodes, for improving the performance. But still, the MICs, mainly NICs and KICs, are in their infancy stage, with many limitations for practical application.

Graphite is considered the most common anode in commercialized LIBs and LICs due to its superior performance characteristics, such as high theoretical capacity (372 mAh g^{-1}), low redox potential ($\sim 0.1 \text{ V vs Li}$), and steady discharge curve.^{23,24} Moreover, it has the unique capability to host a large variety of intercalants. The layered structure of graphite consists of either hexagonal ABAB stacking (Bernal) or rhombohedral ABCABC stacking with a robust covalent bond within the graphene planes. The graphene layers with an interlayer spacing of 3.35 \AA are kept together by the delicate van der Waals forces. Insertion of positively charged alkali metal ions into graphite results in graphite intercalation compounds (GICs), which act as anode materials when the insertion potentials are close to the reduction potentials of alkali metals.²³ A battery-type anode material in which charge-storage occurs by an intercalation reaction curtails structural deviations, which is an imperative condition for achieving a long lifespan in MICs. At the same time, alloying- and conversion-type anodes undergo significant volumetric changes during charge–discharge cycles, which can cause electrode failure upon prolonged cycling.²⁵ Thus, a graphite electrode

based on intercalation chemistry is considered as the top choice for the LIC anode.

Despite the suitability of graphite as anode for LIC, it is tough to consider it for NIC or KIC perspectives. Thermodynamic aspects revealed that the nature of chemical bonding between alkali metal ions and carbon atoms in the graphite strongly influences the metal-ion-storage capacity of the graphite anode.²⁶ Subjected to Li^+ -ions, the graphite lattice can form the stoichiometry of LiC_6 with a theoretical specific capacity of 372 mAh g^{-1} , but for Na and K, it forms NaC_{64} and KC_8 phases with maximum capacity of 35 and 279 mAh g^{-1} , respectively.²³ Theoretical studies proved that the strong local interaction between Na^+ and carbon planes destabilizes the GICs, resulting in a low Na-storage capacity of graphite. It was also reported that Na-GICs were found to be unstable for all intercalation stages. Surprisingly, during 2014–2015, two research groups (Kim et al. and Jache and Adelhelm²⁹) separately found that Na^+ can be reversibly deposited in graphite with high capacity via the solvent co-intercalation reaction. During this reaction, solvated Na-ions are inserted into the space between graphene sheets, forming ternary GICs (*t*-GICs) in place of binary GICs (*b*-GICs) in the conventional intercalation mechanism.³⁰ Inspired by the concept and technical importance of co-intercalation, solvated-ion intercalation of different ions, their electrochemical performance, and the assembly of batteries and hybrid capacitors have been studied in the recent past.^{31–33}

In this work, we summarize the research progress in the field of co-intercalation-based MICs using graphite as the battery-type electrode. The solvated-ion intercalation behavior of Li-, Na-, and K-ions in graphite in the presence of a glyme-based electrolyte will be analyzed, with reported configurations having the respective metal as a counter electrode. We also aim to convey the advantages and challenges of co-intercalation-based battery-type electrodes in place of conventional intercalation-type electrodes for the assembly of MICs with AC as a cathode. Last, we will also discuss the current limitations, lasting encounters, and future prospects of co-intercalation-based MICs.

■ MECHANISM OF CO-INTERCALATION IN GRAPHITIC CARBON MATERIALS

Intercalation vs Co-intercalation Mechanism. Intercalation occurs when atoms or molecules undergo reversible insertion into a layered host structure that contains an interconnected system of empty sites of suitable size. During the insertion of alkali metal ions (AMIs) between graphene planes, the structural integrity of the graphite is conserved.³⁴ At the same time, spacing is expanded to accommodate the guest species, and the reaction is the prototype of the two-dimensional topotactic reaction 1.



As a result of this reaction, pristine graphite becomes AM-GIC. These GICs are the key to explaining the electrochemical performance of the material. Thus, graphite intercalation preserves the structural skeleton of the graphite and causes no breaking of strong chemical bonds, and hence occurs via low energy consumption with a modification of interplanar distance along the *c*-axis. The intercalation mode can be categorized into two types, based on the involvement of solvent in the intercalation (Figure 1a). During conventional

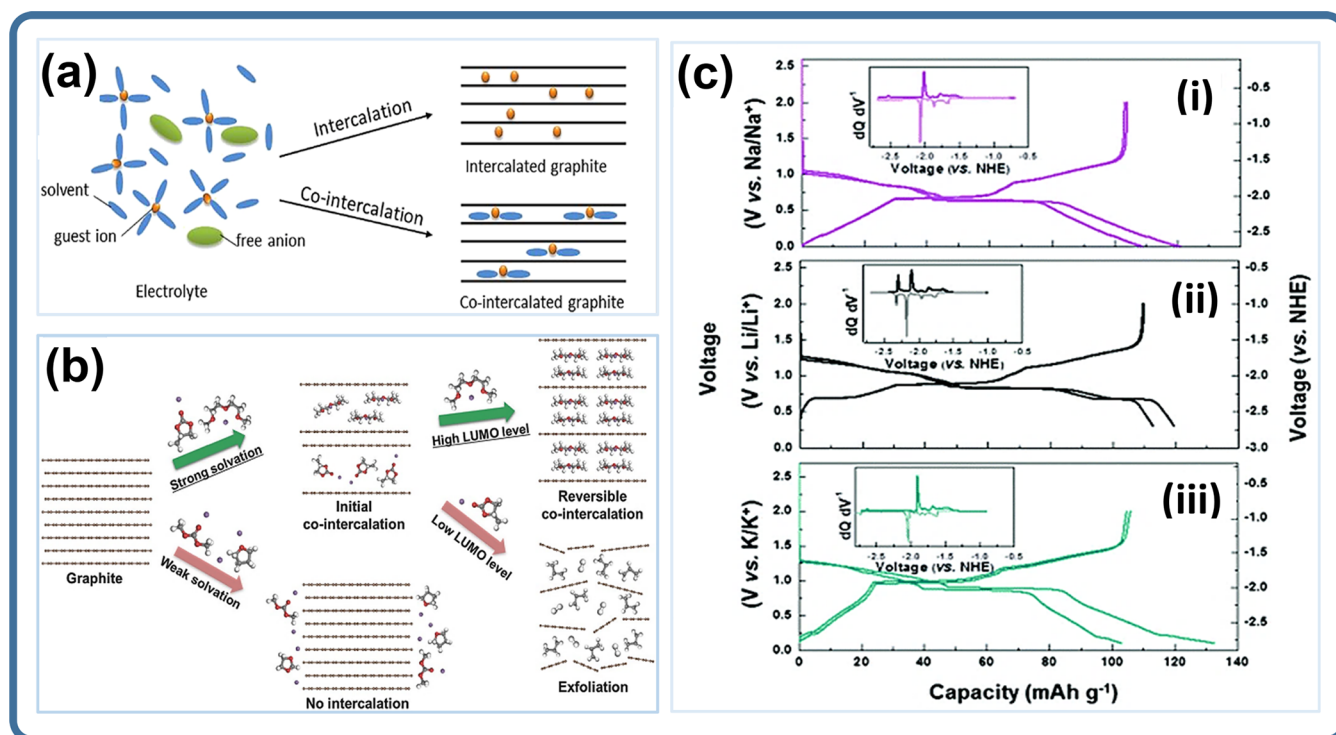
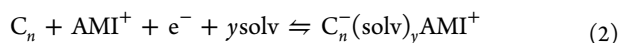


Figure 1. (a) Schematic representations of intercalation and co-intercalation in graphite. Reprinted with permission from ref 30. Copyright 2020 The Authors under a Creative Commons Attribution 4.0 International License, Published by Frontiers Media SA. (b) Graphic design of the conditions for reversible Na co-intercalation. Reprinted with permission from ref 36. Copyright 2016 John Wiley and Sons. (c) Typical co-intercalation charge–discharge profiles of graphite anode with DEGDM electrolyte in half-cell configuration (inset: dQ/dV vs voltage plots for graphite). Reprinted with permission from ref 33. Copyright 2016 Royal Society of Chemistry.

intercalation (eq 1), the insertion of pure guest ions results in the formation of *b*-GICs, which entails stripping of the solvation shell in the reaction.³⁵ But in some cases, solvent molecules intercalate along with guest ions (co-intercalation) into the host lattice structure and form *t*-GICs (eq 2).



In eq 2, “solv” represents the solvent molecule, and $C_n^-(\text{solv})_y\text{AMI}^+$ represents *t*-GIC. However, this co-intercalation is generally considered to negatively impact the cycle life of Li/graphite cells, owing to the decay of co-intercalated solvent in unbalanced *t*-GICs and exfoliation of graphite electrodes. Since 2014–2015, the co-intercalation phenomenon has gathered new consideration in EES devices due to the successful application of reversible solvated Na-ion intercalation. Theoretical studies proved that the development of Na-

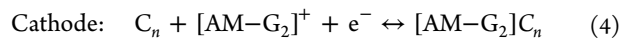
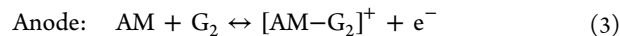
The intercalation mode can be categorized into two types, based on whether the solvent participates in the intercalation or not.

rich *b*-GICs is thermodynamically unfavorable due to strong interaction between graphene layers and Na^+ -ions, which destabilizes the formation of GICs.²⁶ Later it was identified that, in co-intercalation, the presence of solvent enriches the bonding in *t*-GICs, and rebalancing of these bonds occurs via co-intercalation chemistry. The reversibility of solvated-sodium-ion intercalation over hundreds of cycles in the presence of diglyme (G_2) as electrolyte solvent was first

reported by Kim et al.²⁷ They also described that solvated-ion intercalation of AMIs occurs via a fast-staging phenomenon. For different AMIs (Li, Na, and K), their electrochemical properties, such as the shape of the charge–discharge profile and relative location of voltage plateau, remain the same, revealing a common reaction mechanism. Despite the difference in solubility limits of different AMIs in graphite and varying atomic weights, comparable specific capacities were observed.³³

Co-intercalation Voltage. The co-intercalation reaction potential can be represented by considering the reactions involving alkali metal (AM), solvent molecule, and host graphite. The electrode–electrolyte interface reactions for a graphite half-cell with 1 M solution in G_2 solvent can be generally represented as

Graphite electrode||Co-intercalation electrolyte||Alkali metal



where $[\text{AM}-G_2]^+$ represents solvated AMI, and $[\text{AM}-G_2]C_n$ represents *t*-GIC. Based on eqs 3 and 4, solvated intercalation reaction voltage can be written as

$$V = (E_{t\text{-GIC}}^0 - E_{\text{AM}}^0) + \frac{2.303RT}{nF} \log a_{G_2} \quad (5)$$

Here, $E_{t\text{-GIC}}^0$ and E_{AM}^0 denote the standard electrode potentials of *t*-GIC and AM, R symbolizes the universal gas constant ($8.314 \text{ J mol}^{-1} \text{ K}^{-1}$), T designates absolute temperature (K), F denotes the Faraday constant (96485 C mol^{-1}), and a_{G_2} represents the activity of the solvent. Thus, the co-intercalation

potential may vary with the nature of the solvent, the concentration of electrolyte/activity of solvent, and the reaction temperature, and also with the potentials of both graphite and the metal electrode.³² Generally, the co-intercalation potentials are in the 0.5–1 V range, which is much higher than for bare-ion intercalation. Thus, the insertion potentials of solvated AMIs are different and are correlated with the distance between graphene layers in *t*-GICs. A larger ion-induced interplanar space can minimize the repulsive force between negatively charged graphene planes in the discharged condition and cause a higher co-intercalation potential. The relative stability of solvent co-intercalation into the graphite host can be foreseen from the co-intercalation voltage. Moreover, the typical voltage of the graphite electrode increases when larger ions are intercalated (Li < Na < K). A large ion can most efficiently stabilize the host graphite in a discharged condition, leading to a higher co-intercalation potential.³⁶ The co-intercalation voltage or metal-ion-storage potential in co-intercalation increases with an increase in chain length of solvent species; this shows the solvent dependence of the co-intercalation reaction.²⁸

Type of Solvent. The solvated-ion-intercalation mechanism hinges on the type of solvents in the electrolyte, as the structure of *t*-GIC depends on the type of solvent. Glymes (glycol diethers), which are saturated linear ethers, can act as electrolyte solvents instead of commonly used carbonate mixtures and enable energy-storage via the co-intercalation mechanism.^{37,38} Glyme family solutions are usually more environmentally friendly than other organic solvents, as they are less toxic. Moreover, they are less volatile, are chemically and thermally stable, and can form complexes with metal ions.³⁹ The strong solvation of metal ions by linear ethers is due to the multiple oxygen atoms in their structure stabilizing the metal ions.³⁶ The coordination structure of AMIs depends on the type of the co-intercalating solvent molecule. The coordination number, CN (number of molecules in the first coordination sphere), of one AMI in the electrolyte with glyme-based solvent varies from 4 to 7, and complexes with different CN form with different structures.^{28,30} The CN of different glymes and their solvation behavior can be determined by infrared spectroscopy combined with density functional theory (DFT) calculations. Isothermal microcalorimetry can be used for measuring the enthalpy of dissolution for different solvents. Kang's research group²⁸ described the mechanism of Na-storage in graphite using different ether-based electrolytes, including dimethyl ether (DME, monoglyme, G₁), diethylene glycol dimethyl ether (DEGDME, diglyme, G₂), and tetraethylene glycol dimethyl ether (TEGDME, tetraglyme, G₄). Xu et al.³² investigated different factors disturbing the co-intercalation potential of graphite. This reduction potential varies from 0.6, 0.66, and 0.77 V vs Na for G₁, G₂, and G₄ solvent-based electrolytes. They concluded that the average co-intercalation potential upsurges as the chain length of the solvent increases, as a solvent with a longer chain delivers a more effective screening counter to a negative interaction between Na⁺ and host. Yoon et al.³⁶ studied the role of the solvent molecule in maintaining the thermodynamic stability of *t*-GIC and suggested two criteria for solvent selection (Figure 1b): (1) considerable solvation energy that improves the stability of the metal [Na-solvent]⁺ complex and (2) high lowest unoccupied molecular orbital (LUMO) level of [Na-solvent]⁺ complexes which otherwise cause electrolyte decomposition and gas evolution.

But later, Peljo and Girault⁴⁰ revealed that the LUMO or HOMO (highest occupied molecular orbital) of solvent alone could not fix the electrochemical stability window of the electrolytes. However, there is a strong relation between solvent species and co-intercalation behavior that is important to attain efficient storage of metal ions. Using linear ethers as an electrolyte, AMI complexes form, which can be reversibly inserted inside the graphite electrode via a solvated-ion-intercalation mechanism.⁴¹ However, the electrochemical properties of graphite electrodes in Li, Na, and K half-cells undergoing co-intercalation were reported to be similar in terms of the general shape and the position of the voltage plateau, indicating a similar reaction mechanism³³ (Figure 1c).

The co-intercalation mechanism strongly depends on the nature of solvents in the electrolyte, as the structure of *t*-GIC depends on the type of solvent.

Solvation phenomena can be studied with a combination of computational modeling and spectroscopic techniques.^{42,43} G₁, G₂, and G₄ are the most studied solvents for co-intercalation mechanisms. The viscosity of solvents affects the mobility of ionic species within the electrolyte, and it follows the order G₄ > G₂ > G₁. Viscosity is directly associated with the diffusion of ionic species within the electrolyte near the electrode surface. DFT, Fourier transform infrared spectroscopy (FT-IR), and calorimetric studies proved that the chelating ability of glymes increases as the chain length increases. The solvation/desolvation kinetics of different glymes can also affect the electrochemical performance in co-intercalation-based cells. The donor numbers (DN) gives an idea about the solvent's metal-ion affinity (Lewis basicity). Nucleophilic solvents exhibit high donor numbers (DN > 1), and apolar solvents reveal DN values around zero.^{44,45} The DN of glymes falls within the range of 14.0–24.0 kcal mol^{−1}, and the value generally decreases with an increase in chain length.^{41,42} Table T1a in the Supporting Information shows the critical physicochemical properties of these solvents, and Table T1b compares some of their important properties. Besides, G₃ (triglyme) and G₅ (pentaglyme) were also tested as co-intercalation solvents. The performance of G₃ is observed to be different, with a lower capacity discharge profile and ill-defined cyclic voltammogram (CV), and it is understood that solvated-ion intercalation of graphite in the presence of G₃ solvent is only partially reversible.³² The reason behind the poor performance of G₃ was reported as steric hindrance, but it remains uncertain that this performance failure is due to thermodynamic or kinetic reasons. The performance of G₅ for graphite co-intercalation has been tested for the first time by Adelmhelm's research group.⁴⁶ They reported that G₅ could only exhibit low capacity with large polarization at room temperature. Moreover, they studied the suitability of crown ethers as co-intercalation solvent. The thermodynamic stability of *t*-GICs depends on three factors: (i) the interaction between intercalants and graphene planes, (ii) force of repulsion between positively charged intercalant species, and (iii) the repulsive force between negatively charged graphene layers.^{32,33} When the chain length of the solvent grows, the metal ions are more effectively protected within the solvation

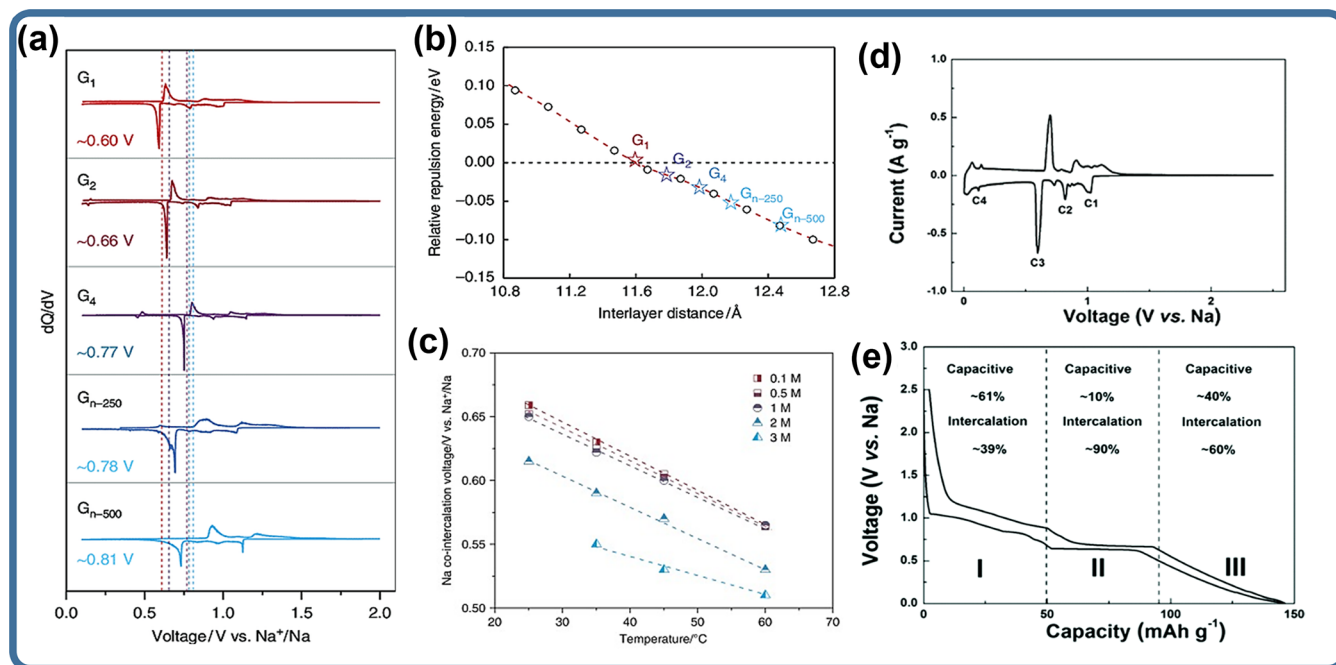


Figure 2. Solvent and temperature dependence of co-intercalation voltage and capacitive contribution in the total charge-storage mechanism. (a) Variation of co-intercalation potential with respect to glyme length; dQ/dV plots of graphite electrodes cycled in G_1 , G_2 , G_3 , G_4 , G_{n-250} , and G_{n-500} electrolytes. (b) Normalized repulsion energy vs interlayer distance plot to explain the variation in Na-storage potential in graphite based on the type of ether. (c) Na co-intercalation voltage in graphite at different concentrations of G_2 -based electrolytes as a function of operating temperature. Reprinted with permission from ref 32. Copyright 2019 The Authors under a Creative Commons Attribution 4.0 International License, Published by Springer Nature. (d) CV profile of natural graphite to examine Na-storage behavior during co-intercalation. (e) Typical charge–discharge profile with quantitative contributions of capacitive and intercalation Na-storage determined using power-law relationship. Reprinted with permission from ref 27. Copyright 2014 John Wiley and Sons.

sphere, and hence the interaction among intercalants and graphene planes is minimized, thus causing stabilization of t -GICs and a rise in co-intercalation potential. Therefore, longer ether solvent molecules result in higher co-intercalation voltage, and the force of repulsion between the graphene planes in t -GICs can be relieved by larger interlayer distances offered by solvated-ion intercalation.³²

Concentration of Electrolytes. Xu et al.³² studied the solvent activity dependence of solvated-ion-intercalation voltage, and they suggested that the free solvent activity in the electrolyte ($I_{\text{solvated}}/I_{\text{free}}$) can be abridged by considering extremely concentrated electrolytes, which in turn lessen the average co-intercalation potential. As the concentration of electrolytes increases, the Na/AM-storage potentials shift to lower values. Thus, highly concentrated electrolytes can be used to tune the co-intercalation voltage, whereas for strong electrolytes above 1.5 M, a substantial reduction of free solvent molecules occurs and was confirmed by FTIR and Raman analysis. The most commonly studied salt systems for co-intercalation reactions include MCF_3SO_3 , MPF_6 , MOTf , and MClO_4 ($M = \text{Li}, \text{Na}, \text{K}$). LiPF_6 has too low solubility in G_2 , which should be considered while selecting salt systems for co-intercalation studies, that help to avoid the unnecessary complications of anion contribution in the solvent intercalation mechanism.³²

Temperature Dependence of Solvated-Ion Intercalation. The studies reported a negative shift in co-intercalation voltage concerning an increase in temperature. The temperature coefficient, $\Delta E/\Delta T$, is found to be -2.85 mV K^{-1} for dilute electrolyte solutions (0.1–1 M) and -1.6 mV K^{-1} for concentrated electrolyte solutions (2–3 M). The difference in

temperature coefficient is ascribed to the reduced activity of free solvent molecules³² and is given by the equation,

$$\frac{\partial E}{\partial T} = \frac{2.303R}{nF} \log a \quad (6)$$

where a represents the activity of free solvent molecules. The temperature coefficient can also be stated in terms of entropy changes (ΔS) during co-intercalation:

$$\Delta S = nF \frac{\partial E}{\partial T} \quad (7)$$

Kang's group suggested that the entropy changes during co-intercalation are orders of magnitude greater than those of conventional bare-ion-intercalation reactions. These entropy changes can be due to the involvement of the liquid-phase reactant (solvent molecule) in the co-intercalation reaction mechanism.³² Goktas et al.⁴⁶ studied the influence of temperature on the electrochemical activity of host graphite during solvated-ion-intercalation reactions using a range of glymes (G_1 to G_5). They reported that for G_1 , G_2 , and G_4 , the electrode reaction is thermodynamically controlled for the whole temperature range (20–80 °C). G_5 showed poor performance at room temperature, but the performance was enhanced at elevated temperatures. The probable reason behind this temperature effect in the co-intercalation reaction is the change in viscosity of the solvent, which is greater at room temperature but diluted at elevated temperature conditions. It was also reported that G_3 shows poor performance compared to other glymes, as the reaction remains kinetically controlled due to lower ideal coordination.⁴¹

Charge-Storage Mechanism. Kang's group²⁷ investigated the charge-storage mechanism in natural graphite during solvated-ion intercalation using a typical CV profile. The presence of several cathodic anodic peaks indicated that multiple electrochemical reactions are taking place during co-intercalation. They quantified the contribution from capacitive- and intercalation-type reactions by means of CV data at different scan rates through the power-law relationship. The study reported the presence of combined intercalation and capacitive reactions during co-intercalation. Figure 2 illustrates the solvent and temperature reliance on co-intercalation potential and the capacitive contribution in the total charge-storage mechanism.

CO-INTERCALATION KINETICS

The kinetics of co-intercalation is unusually quicker than that of conventional intercalation reaction. Ether-based electrolytes can act as co-intercalation electrolytes, as they are capable of causing solvated-ion (Na^+) intercalation into graphite. In contrast, ester-based electrolytes can only transfer the Na^+ -ions from the bulk electrolyte solution to the storage site on the electrode without direct involvement in intercalation, as the ions are desolvated before entering into the host lattice. But this desolvation process is absent in the case of solvated-ion intercalation. Moreover, this is considered the foremost rate-deciding step in the charge-transfer process. Ether-based electrolytes have unique solvating properties and are more resistant to reductive decomposition, leading to the formation of a marginal solid–electrolyte interphase (SEI) on the anode side, and thus offer higher initial coulombic efficiency (ICE) in comparison with ester-based electrolytes.³⁸ These studies concluded that the absence of the desolvation step during the solvated-ion intercalation and the thinner SEI layer on the graphite anode together promoted the co-intercalation kinetics.⁴⁷ In addition, the lessened interaction between solvated-ion and graphene planes also contributes to the speedy diffusion of solvated ions in graphite lattice.

ELECTROCHEMICAL ACTIVITY OF GRAPHITE WITH ALKALI METAL (Li/Na/K) CELLS

Different AMIs (Li, Na, and K) can be inserted with solvated shells into graphite host when co-intercalation-based solutions are used. The co-intercalation of each AMI exhibits a fast-staging phenomenon irrespective of AMI species. When the size of the cation increases, $\text{Li} < \text{Na} < \text{K}$; interlayer distance increases proportionately, decreasing the repulsion between graphene layers with a negative charge in the discharged condition. Hence, for the larger t -GIC, there will be abridged repulsion between the graphene layers, which will have higher AMI-storage potential. The insertion behavior of AMIs, including specific capacity, remains similar. In contrast, the co-intercalation potential can be related to interplanar space in the intercalated graphite host (11.16, 11.65, and 12.11 Å for Li, Na, and K AMIs, respectively).^{33,48} Bader charges, representing the charge carried by an atom, were calculated as +0.88, +0.85, and +0.88, corresponding to solvated Li-, Na-, and K-ions, respectively. Moreover, they exhibit similar charge–discharge profiles regarding the shape and position of the voltage plateau, representing a common reaction mechanism with graphite.⁴¹

Li/Graphite Cells. Intercalation of solvated Li-ions or the co-intercalation concept for Li-ions was reported upon the discovery of Na co-intercalation reactions. But it was regarded

as undesirable, as it can trigger the graphene layer's exfoliation and thus cause the destruction of graphite's crystal structure, causing the cell to fail due to poor cycle life. Hence, for the graphite anodes in LIBs, the co-intercalation concept was regarded as harmful to the system. The first reversible solvated Li-ion insertion in graphite was reported by Abe et al.⁵⁰ They used solvents having high donor numbers (monoglyme, DME; dimethyl sulfoxide, DMSO) in the electrolyte and observed moderately reversible co-intercalation with oxidation–reduction peaks that differ from those of conventional simple Li-ion intercalation with solvent decomposition. Yamada et al.⁵¹ stated that, by changing the salt concentration, the solvation number of the solvent molecule for Li-ions could be managed for Li-ion co-intercalation. In 2016, Kim et al.³³ successfully established the electrochemical performance of Li/graphite co-intercalation cells using G_2 solutions. The cell could deliver a discharge-specific capacity of $\sim 100 \text{ mAh g}^{-1}$ at a constant current rate of 0.010 A g^{-1} . The specific capacity value, structural progress, and staging phenomenon were comparable to those of Na- and K-based co-intercalation cells.³³

Later, Kim et al.^{33,52} further examined the Li-ion solvated-ion-intercalation phenomenon in graphite, using 1 M lithium trifluoromethanesulfonate (LiTF) in G_2 . The charge–discharge profiles and specific capacities were similar to those in previously reported studies. However, a decrease in specific capacity was observed with repeated cycling. Only a fraction of the initial capacity was observed after 20 charge–discharge cycles, indicating less stability of solvated Li-ion intercalation-based graphite cells. The authors reported that the main reason for this cycle degradation of Li co-intercalation was linked to side reactions at the counter Li electrode surface rather than the co-intercalation process. Side reactions occur mainly due to chemical incompatibility between Li metal and G_2 electrolytes. They also suggested that the structural degradation of the graphite host lattice does not happen in Li/graphite co-intercalation-based cells. The cycle stability was significantly enhanced by lithium nitrate additive, forming a protective layer on the Li metal surface, contrary to the electrolyte. Moreover, the study showed that the co-intercalation-based reaction could provide higher power capability than conventional Li-ion intercalation. Co-intercalation of solvated Li-ion into graphite could be executed up to 1 A g^{-1} with a charge time less than 6 min without any substantial capacity diminishing. At the same time, the capacity values were nearly constant, regardless of current applied, and even surpassed that of bare Li-ion intercalation for current rates higher than 0.5 A g^{-1} . This is due to the low polarization values of co-intercalation-based cells at high current rates. It shows the suitability of graphite Li-co-intercalation-based cells for high-power applications with increased safety. Conventional Li-ion intercalation-based graphite cells can cause safety-related issues during the fast lithiation process, as Li metal plating due to overpotential developed at high currents. Fast solvated-ion-intercalation kinetics of co-intercalation can prevent such safety issues, and a high working potential ($>0.3 \text{ V vs Li}$) impedes Li metal plating. Besides, the sizable interplanar distance in graphite generated because of initial co-intercalation of the $[\text{Li-ether}]^+$ complex helps in subsequent charge–discharge cycles with non-limited-diffusion kinetics. So, $[\text{Li-ether}]^+$ solvated-ion intercalation shows a capacitive performance with a speedy charge-storage mechanism.

The high-power density of Li/graphite solvated-ion intercalation-based cells can be credited to faster desolvation

kinetics, marginal SEI layer on the graphite anode, and diffusion-less charge-storage mechanism. Improved safety and increased power capability point out the options for using co-intercalation-based Li/graphite cells in various energy-storage devices. However, solvated-ion intercalation is believed to have adverse impacts on the cyclic stability of Li/graphite cells, owing to the combined effect of co-intercalated solvent molecule decomposition in *t*-GICs and subsequent exfoliation of graphite electrode.²³

Na/Graphite Cells. Graphite was alleged to fail application as an anode material for Na-based systems, as only an insignificant amount of Na⁺-ions can be inserted into the graphite (30 mAh g⁻¹). This was due to the thermodynamic instability of *b*-GICs, based on computational studies. In 2014, Jache and Adelhelm⁵³ showed that this issue could be bypassed by the solvated-ion-intercalation phenomenon in a diglyme-based electrolyte. The resultant GIC was a stage 1, *t*-GIC with predicted geometry of Na(diglyme)₂C₂₀ graphite. The researchers reported that the reaction showed a slight irreversible capacity loss in the first cycle. A specific capacity close to 100 mAh g⁻¹ with excellent cyclic stability over 1000 cycles with >99% coulombic efficiency was observed. They proposed that the co-intercalation-based graphite electrodes could be used for small and stationary applications. During the same period, Kang's group^{27,28} explained that graphite could also act as an outstanding anode for NIBs. A graphite anode in G₂ delivered a reversible capacity of 150 mAh g⁻¹ with cyclability over 2500 cycles at a current density of 0.1 A g⁻¹. The cells also displayed an excellent rate capability of 75 mAh g⁻¹, even at 10 A g⁻¹ current input. The group also observed that the co-intercalation voltage could be altered from 0.6 to 0.78 V vs Na by varying the chain length of the electrolyte. Ether-based solvents with high donor numbers result in the formation of stable *t*-GICs with non-polar characteristics. They could also suppress electrolyte decomposition, which leads to a marginal SEI layer formation on the graphite surface. The researchers confirmed that co-intercalation is possible with G₂ and other ether-based electrolytes, G₄ and G₁, and solvents with elongated chain lengths form dynamically more steady discharged products displaying a higher Na-ion-storage potential. In comparison, they stated that G₂ shows superior rate capability. They also identified the partial pseudo-capacitive behavior in the solvated Na-ion-intercalation mechanism. They proposed that the solvated Na⁺-ions, [Na-ether]⁺ complexes, double stacked in parallel with graphene planes in the graphite host lattice. The relation between solvent type and co-intercalation phenomenon recommends the possibility of tuning Na-storage behavior in graphitic materials.

Motivated by these findings, Yoon et al.³⁶ studied the solvent dependence of co-intercalation through a systematic investigation. They concluded that the high *E*_s of Na and chemical firmness of Na-solvent complexes are essential for reversible co-intercalation. Jung et al.⁴⁷ demonstrated that graphite exhibits an unrivaled rate capability and cyclic stability for Na⁺ solvent co-intercalation. The diglyme-graphene van der Waals interaction supports the interlayer coupling strength and advances graphite exfoliation resistance. The flat diglyme molecules that solvate Na⁺-ions can move swiftly in the interlayer region of graphite, resulting in Na-diglyme co-diffusion which is 5 times faster than Li⁺-diglyme co-diffusion. Later, Goktas et al.³¹ used different techniques like online electrochemical mass spectrometry (OEMS), scanning elec-

tron microscopy (SEM), transmission electron microscopy (TEM), and X-ray diffraction (XRD), as well as theoretical knowledge to improve the knowledge of co-intercalation mechanisms. They reported that the reaction is highly reversible, as the graphite particles only exfoliate to form crystalline platelets rather than delaminate. Dilatometry studies displayed that intercalation reaction occurs at a voltage plateau of 0.6 V vs Na, whereas for potentials below 0.5 V vs Na, the reaction behavior is more pseudocapacitive than Faradaic. They also pointed out that the reaction is possibly the first illustration of the use of a SEI-free graphite anode material. In another work, the same research group⁴⁶ studied the influence of temperature (20–80 °C) on the electrochemical activity of graphite electrodes undergoing co-intercalation reactions in Na-cells. They found that many solvents unsuitable for a co-intercalation mechanism, such as G₅ at room temperature, became suitable at elevated temperatures. At the same time, parasitic reactions were found to appear in high-temperature conditions. The scientists concluded that temperature is an essential parameter for solvated-ion-intercalation reactions as they can be triggered by temperature.

K/Graphite Cells. The richness of potassium resources and the low working potential of K⁺-ions in organic electrolytes (−2.93 V vs SHE) make potassium-based energy-storage devices potential candidates for future energy-storage. But the main challenge is to find a suitable electrode material, owing to the large ionic size of K⁺ (1.38 Å) in comparison with Li⁺ (0.76 Å). In 2015, Ji's group⁵⁴ reported the electrochemical K⁺ insertion in graphite using 0.8 M KPF₆ in ethylene carbonate (EC)/diethyl carbonate (DEC) solution. The study presented a reversible capacity of 273 mAh g⁻¹, representing stage-1 *b*-GIC (KC₈). But the cell exhibited poor rate capability (80 mAh g⁻¹ @ 1C) and cyclic instability (50.8% of initial capacity after 50 cycles), which hindered the practical application of K-based systems. In 2016, Pint's research group reported the first demonstration of K⁺-ion co-intercalation into graphite.⁵⁵ Potassium/KPF₆ in a diglyme/graphite cell unveiled a reversible capacity of 100 mAh g⁻¹ (@ 0.2 A g⁻¹), with 95% capacity retention over 1000 charge–discharge cycles. Moreover, the cell could exhibit >99% coulombic efficiency and decent rate capability (80% up to 10 A g⁻¹). The authors correlated this result with factors such as lack of desolvation step and weak lattice–host interaction. Raman and XRD analyses confirm no defect formation or damage in the crystalline structure of graphite, even after 1000 cycles of solvated K⁺-ion intercalation/de-intercalation. The researchers could also observe the sequential appearance of stages from 4 to 1, and in a charged stage-1 *t*-GIC, there was a lattice expansion from 0.335 to 1.16 nm, with a work function of 3.4 eV. In the same year, Kang's group³³ made a comparison study of solvated-ion-intercalation behavior of Li, Na, and K in graphite. They stated that the specific capacity and insertion behaviors remain the same, and only the intercalation potential changes with interplanar distance in the intercalated host gallery. Similar discharge capacities were observed for all the three AMIs, which conflicted with the substantial solubility limit of each AMI into graphite and their atomic weights. Slightly enhanced irreversible capacity was detected for Na and K in comparison with Li. The electrostatic impact between negatively charged graphene planes in the discharged state and its delicate disparity with interlayer distance is the leading reason for the different voltages detected for Li, Na, and K insertion. According to the group, the development of K-

Table 1. Comparison of Essential Characteristics of Li, Na, and K and the Electrochemical Properties of the Co-intercalating Electrode^{23,32,49}

	Li	Na	K
atomic number	3	11	19
electronic configuration	[He]2s ¹	[Ne]3s ¹	[Ar]4s ¹
atomic weight (g mol ⁻¹)	6.941	22.989	39.098
number of valence electrons	1	1	1
Pauling electronegativity	0.98	0.93	0.89
abundance in the Earth's crust (%)	0.0017	2.36	2.09
price (\$ kg ⁻¹)	17.00	0.15	0.74
density (g cm ⁻³)	0.534	0.968	0.89
melting point (°C)	180.54	97.72	63.38
ionic radius (Å)	1.45	1.80	2.20
std reduction potential against SHE (V)	-3.04	-2.71	-2.93
gravimetric capacity (mAh g ⁻¹)	3829	1165	685
volumetric capacity (mAh cm ⁻³)	2062	1131	591
ionic radius (for metallic cation) (Å)	0.76	1.02	1.38
Stokes radius (Å) in PC	4.8	4.6	3.6
Stokes radius (Å) in water	2.38	1.84	1.25
potential window in carbonate ester solvents (V)	4.5	4.2	4.6
metal plating voltage (V) vs Li	0	0.3	-0.1
Electrochemical Properties of the Co-intercalating Graphite Electrode in 1 M MCF ₃ SO ₃ (M = Li, Na, or K) Salts in DEGDMC ³³			
interlayer distance (Å)	11.16	11.65	12.11
average voltages of graphite in alkali-ion cells/ stability of co-intercalated graphite	-2.054 V vs NHE	-2.024 V vs NHE	-1.961 V vs NHE (more stable than Li and Na counterparts by 93 and 63 meV, respectively)
Badger charges (amount of charge carried)	+0.88	+0.85	+0.88
discharge capacity (mAh g ⁻¹)	~115	~110 (with slightly increased irreversible capacity)	~100 (with slightly increased irreversible capacity)
cycle stability of graphite electrode	rapid capacity degradation	97% retention after 60 cycles compared to the second cycle	91% retention after 60 cycles compared to the second cycle

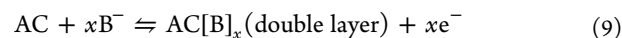
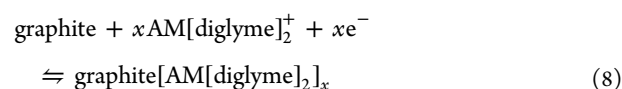
intercalated graphite is believed to be more steady and energetically more favorable than that of Li- or Na-intercalated *t*-GICs by 0.093 and 0.063 eV, respectively. Wang et al.⁵⁶ compared K-ion insertion into graphite in ester- and ether-based solvents by considering thermodynamic and kinetic behaviors. They reported that ether-based electrolytes, due to a charge shielding effect, offer a high working potential (0.7 V vs K) in comparison with carbonate-based electrolytes (0.2 V vs K). Along with good rate performance, thin SEI layer formation, a slight volume increase of <10% (from 3.36 to 3.62 Å for the (002) plane), and an apparent diffusion rate of 10⁻⁸ cm² s⁻¹ are noteworthy. Li et al.⁵⁷ specified that the main reason for wild kinetics is the absence of a passive desolvation process. They also analyzed the role of wettability between the electrode and electrolyte on electrochemical performance. They stated that good electrolyte wetting could guarantee faster ionic transfer throughout the cycling process. These reports suggest that graphite can be effectively used as a co-intercalation-type anode for high-performance charge-storage devices. A comparison of essential characteristics of Li, Na, and K and the electrochemical properties of the co-intercalating electrode are listed in Table 1.

■ CO-INTERCALATION-BASED MIC

The MIC benefits from the use of electrochemical capacitor technology (EDLC electrode) and the AMI-based battery concepts. The overall working mechanism of the hybrid device will be the combination of both, and it will be trickier. This concept is developed to achieve both high energy and high

power in a single device. Several factors affect the charge-storage processes and the mobility of ions between the two electrodes and, eventually, the performance of this device.⁶⁴ Co-intercalation-based MIC consists of one EDLC electrode and one co-intercalation-based battery-type electrode. In this part, we summarize the research works reporting for the assembly of MICs with a co-intercalation-type battery anode and an AC cathode in the presence of a glyme-based electrolyte. MICs comprising solvated monovalent ions for the bulk diffusion activity comprise Li, Na, and K-ion capacitors based on co-intercalation, in which Li-glyme⁺, Na-glyme⁺, and K-glyme⁺ ions move to and fro through the glyme-based solvent.

The half-cell reactions for a MIC with diglyme-based electrolyte can be represented as



Equations 6 and 7 represent reactions at battery-type and capacitive-type electrodes, respectively. AM represents a cation/alkali metal ion (Li, Na, or K), and B represents the anions present in the electrolyte solution. During charge, solvated AMIs are relocated from the electrolyte solution to the negative graphite electrode (co-intercalation), and anions from the electrolyte move to the AC positive electrode (electrochemical double-layer formation) simultaneously.

Table 2. Comparison of Co-intercalation vs Conventional Intercalation of Li, Na, and K

	co-intercalation		conventional intercalation	
nature of electrolyte	ether-based		carbonate ester-based	
GIC formed	ternary		binary	
nature of SEI layer	thin/absent (forms and breaks/dissolves due to volume expansion) ³¹		thick (up to 100 nm) ³¹	
rate capability	high		low	
de-solvation step	absent		present	
involvement of electrolyte in the electrode reaction	present		absent	
redox potential	high	<ul style="list-style-type: none"> • 0.75 V vs Li • 0.6–0.8 V vs Na • 0.7 V vs K 	low	<ul style="list-style-type: none"> • 0.15 V vs Li • does not form Na-rich <i>b</i>-GIC • 0.2 V vs K
reversible specific capacity	low	112 mAh g ⁻¹ @ 0.1 A g ⁻¹ (vs Li) ⁵⁸	high	372 mAh g ⁻¹ (LiC ₆ formation)
	high	118 mAh g ⁻¹ @ 0.05 A g ⁻¹ (vs Na) ⁵⁹	low	35 mAh g ⁻¹ (~NaC ₆₄)
	low	85 mAh g ⁻¹ @ 2 A g ⁻¹ (vs K) ⁶⁰	high	280 mAh g ⁻¹ (KC ₈)
volume/linear expansion	334% along <i>c</i> -axis during Li co-intercalation ⁵² 200–300% for [Na-ether] ⁺²⁸ <10% (3.36 to 3.62 Å for (002) plane) for K ⁵⁶		13% from 3.35 to 3.7 Å ²³ — 63% from pristine 3.36 to 5.49 Å ⁵⁶	
diffusion coefficient	high	Li ⁺ -ion 4.8 × 10 ⁻⁴ cm ² s ⁻¹ (anodic) 6.2 × 10 ⁻⁴ cm ² s ⁻¹ (cathodic) (Randles–Sevsik equation) ⁵⁸ Na ⁺ -ion 1.73 × 10 ⁻⁷ cm ² s ⁻¹ (anodic) 1.16 × 10 ⁻⁷ cm ² s ⁻¹ (cathodic) (Randles–Sevsik equation) ⁵⁹ (1–6) × 10 ⁻¹⁰ cm ² s ⁻¹ (GITT method) ⁶² K ⁺ -ion 3.0 × 10 ⁻⁸ cm ² s ⁻¹ (Randles–Sevsik equation) ⁵⁶ ~5 × 10 ⁻⁸ cm ² s ⁻¹ (GITT method) ⁵⁶	low	Li ⁺ -ion 10 ⁻⁸ –10 ⁻¹⁰ cm ² s ⁻¹ (PITT method) ⁶¹ Na ⁺ -ion 10 ⁻¹³ –10 ⁻¹⁴ cm ² s ⁻¹ (PITT method) ⁶³ K ⁺ -ion 6.1 × 10 ⁻¹⁰ cm ² s ⁻¹ (Randles–Sevsik equation) ⁵⁶ ~10 ⁻¹⁰ cm ² s ⁻¹ (GITT method) ⁵⁶
diversity of chemistry	high		low	

Table 2 outlines the comparison of co-intercalation vs conventional intercalation of Li-, Na-, and K-based systems.

Li-Ion Capacitors (LICs). LICs are assembled to accomplish higher energy storage capacity than typical EDLC and higher power storage capability than LIBs. They employ a pre-lithiated battery-type anode and a capacitor-type cathode.^{10,12,13,15,65} Considering the previous reports on solvated Li-ion intercalation in graphite lattice, our group recently established the assembly of a dual carbon co-intercalation-based LIC.⁵⁸ The device used 1 M LiPF₆ in G₄ electrolyte, a spent LIB recovered graphite (RG) anode, and a commercial AC cathode. RG acts as a co-intercalation-type battery electrode to intercalate glyme-solvated Li-ions; AC serves as an EDLC-type electrode that undergoes adsorption–desorption of anions on the electrode surface. The dual carbon LIC could deliver maximum energy and power density values of 46.40 Wh kg⁻¹ and 5.64 kW kg⁻¹, respectively, at ambient conditions. This glyme-based LIC could lead to a conventional, carbonated-based LIC with RG anode in terms of cyclability and safety.¹⁶ But the half-cell performance of both anode and cathode showed less stability when pairing with Li metal anode, which can be described by the instability of glyme-based electrolytes in contact with Li metal. On the other hand, the issue was not detected in the LIC assembly due to

the absence of Li metal. The low- and high-temperature performance of fabricated LIC was also studied. The meager performance of LIC at low temperature was explained on the basis of amplified cell polarization due to slow kinetics of solvated ions. The low energy density value of this co-intercalation-based LIC is linked with lower Li-intercalation potential (0.15 V vs Li) in comparison with higher solvated-ion-intercalation voltage (0.75 V vs Li). At the same time, low intercalation potential may lead to Li metal plating and hence affect the device's safety. Therefore, this glyme-based LIC concept can be treated as an appropriate option for low-energy and long-term applications. Further research activities are vital to get the best performance out of this glyme-based LIC concept.

Na-Ion Capacitors (NICs). The idea behind the assembly of Na-based energy-storage devices is to replace Li with Na since Na is electrochemically similar to Li and its source is abundant. Na-based hybrid energy-storage device NICs have attracted much attention in the past decade. The type of electrode material for NICs is significant, as it affects the performance to a great extent.^{21,66–69} Graphite, the state-of-art anode material for LICs, was considered unsuitable for NIC application as Na can hardly intercalate into graphite host lattices. Amazingly, Adelhelm's and Kang's research groups^{28,53}

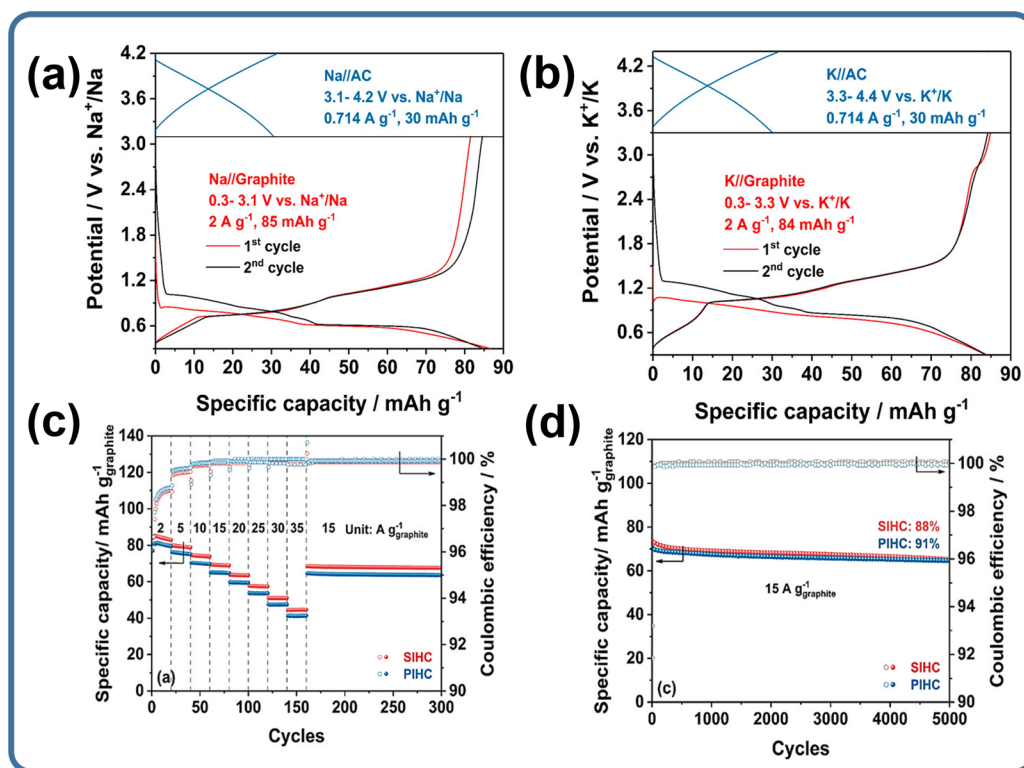


Figure 3. Graphite//AC MICs (Na and K): Charge–discharge curves of graphite and AC electrodes in the three-electrode system: (a) sodium and (b) potassium half-cells. (c) Specific capacity and Coulombic efficiency of NIC (SIHC), and KIC (PIHC) at different current rates. (d) Long-term cycling of the NIC and KIC. Reprinted with permission from ref 60. Copyright 2019 American Chemical Society.

explored whether sodium could reversibly insert into a graphite host using the idea of the co-intercalation phenomenon. By considering the reported works on co-intercalation-based graphite anodes, Han et al.⁷⁰ established a NIC with a sodium-inserted graphitic meso-carbon microbead (MCMB) anode and an AC cathode in a G₂-based electrolyte. The device exhibited a maximum energy density of 93.5 Wh kg⁻¹ at a power of 0.57 kW kg⁻¹. Even at a high-power value of 2.83 kW kg⁻¹, the device delivered 86.5 Wh kg⁻¹ with a capacity retention of 98.3% after 3000 charge–discharge cycles. The researchers pointed out that the performance was superior to that of reported NICs in ester-based electrolytes.

In 2019, Liu et al.⁶⁰ reported the assembly of another intercalation-based NIC prototype, using commercial graphite as a battery-type negative electrode that hosts solvated Na-ions and an AC cathode as EDLC-type electrode in 1 M NaPF₆ in G₂ electrolyte within the potential window of 0–3.9 V (Figure 3). The prototype exhibited very decent cyclic stability, high-rate capability, and high ICE. The fabrication was done without pre-sodiation, and hence, it is highly suitable for practical applications. The device could achieve a maximum power density of 17.13 kW kg⁻¹ with 88% retention after 5000 cycles. In parallel, our group⁵⁹ proposed NIC assembly with RG from spent LIBs as co-intercalation-based anode and commercial AC as EDLC-type cathode in the presence of 0.5 M NaPF₆ in G₄ electrolyte. Interestingly, we found the dominant pseudocapacitance involvement in the total charge-storage mechanism of the graphite anode. The assembled RG (pre-sodiated)//AC could deliver maximum energy and power density values of 59.93 Wh kg⁻¹ and 6.8 kW kg⁻¹, respectively, with 98% capacity retention after 5000 cycles at ambient conditions. After thermal activation, the cell unveiled a very

high energy density of 71.27 Wh kg⁻¹. Moreover, the effect of temperature on the electrochemical performance of the NIC was checked and confirmed that the device could exhibit excellent performance at low- and high-temperature conditions.

The kinetic mismatch between the wild capacitive charge-storage mechanism on the cathode and slow battery-type reaction on the anode usually results in meager rate capability and inadequate power yield from NICs. Huang et al.⁷¹ developed an ultrafast NIC using electrochemically exfoliated graphite (EEG), having improved capacitive energy-storage, as anode and an AC cathode using a co-intercalation-based electrolyte (Figure 4). The EEG anode in the presence of 1 M NaPF₆ in G₄ could produce a high reversible capacity of 109 mAh g⁻¹ and preserve 90% of its initial capacity after 1000 cycles. 2D ultrathin nanosheets of EEG could boost the kinetics of solvated-ion storage compared to graphite electrodes. Besides, a well-stacked EEG film anode with open voids could lessen the volume expansion problems related to solvated-ion intercalation. The formulated NIC could finish the charge–discharge process in <10 s and achieve an ultra-high power density of 17.5 kW kg⁻¹ with an energy density of 17 Wh kg⁻¹. The capacitive contribution from the anode and the capacitive cathode results in wild rate capability and high power output for the assembled co-intercalation-based NIC.

Electrochemical systems with glyme solvents showed good compatibility due to their thinner and stable SEI, higher coulombic efficiency, and faster charge-storage mechanism. But the limited Na-storage property of the graphite anode (~110 mAh g⁻¹) results in low energy-storage capability in the NIC configuration with an AC cathode. In a recent study, Adelhelm's group⁷² discussed synthesizing graphite Sn

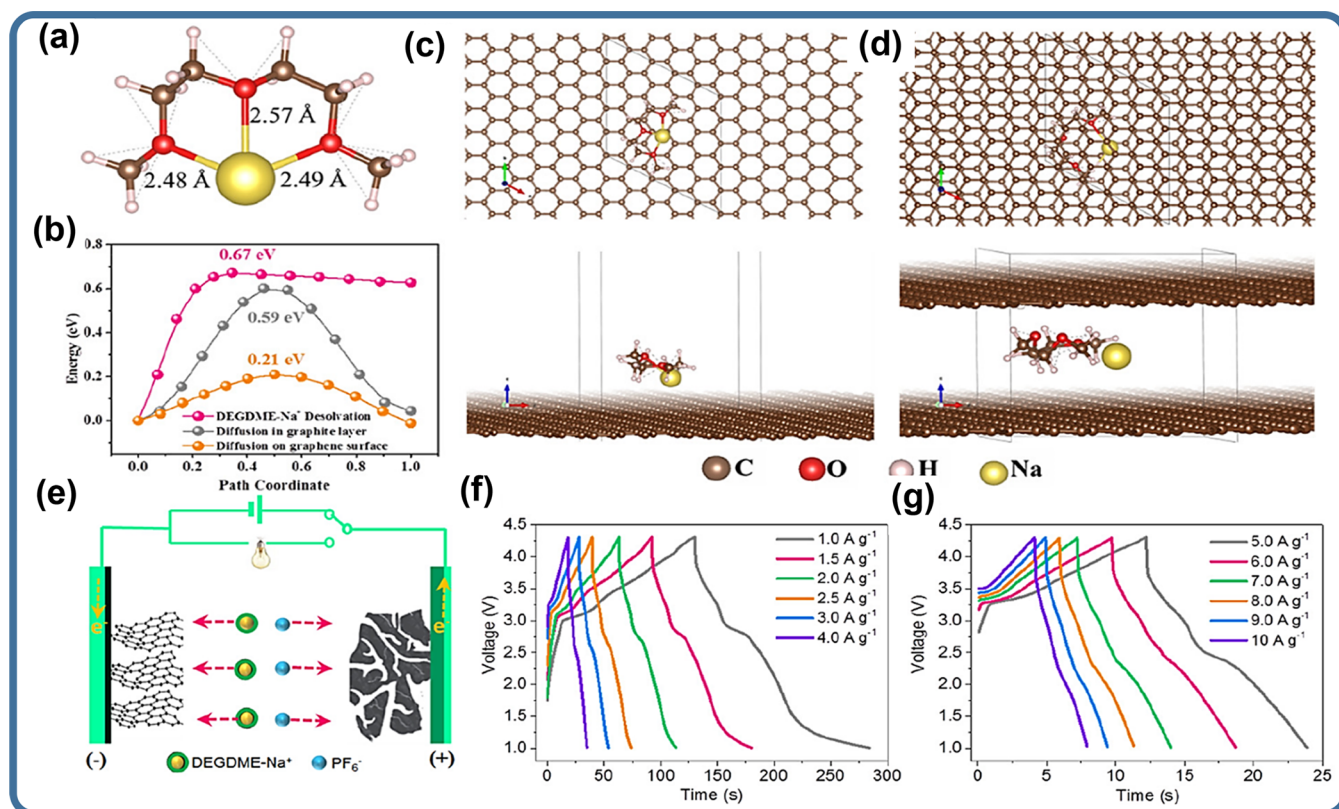


Figure 4. (a–d) Theoretical calculations of Na^+ -DEGDME complex structure and its diffusion on the graphitic material. (a) Optimized structure of the complex. (b) Energy barrier for solvated-ion diffusion on the surface and in the interlayer of graphite. (c) Optimized structure of Na^+ -DEGDME on the graphite surface and (d) in the graphite interlayer. (e–g) Electrochemical properties of the EEG//AC NIC. (e) Schematic representation of the working principle of NIC and (f, g) charge–discharge curves at different current rates. Reprinted with permission from ref 71. Copyright 2020 American Chemical Society.

composite material as Snt-graphite (17 wt% Sn) by annealing SnCl_2 with graphite in an inactive atmosphere (Figure 5). The composite could overcome the limited Na-storage property of the graphite anode. The material delivered a higher specific capacity of 223 mAh g^{-1} with capacity retention of 96% after 2200 cycles. The composite material displayed two different sodium-storage mechanisms, viz. graphite in co-intercalation of solvated Na-ions, and Sn involving the reversible alloy formation. *In situ* XRD and *in situ* electrochemical dilatometry confirmed this. The researchers reported that adding Sn could double the electrode capacity, whereas the influence on electrode expansion was only 3%. The assembled NIC with a Snt-graphite anode and an AC cathode provided a maximum energy and power density of 93 Wh kg^{-1} and 7.8 kW kg^{-1} , respectively, with 80% capacity retention after 8000 cycles. Thus, the composite material could be considered an exciting candidate for high-performance energy-storage devices.

Our group⁷³ recently assembled a NIC with waste-rubber-derived graphitic carbon nanofibers (GCNFs) as a battery-type co-intercalation-based negative electrode and an AC positive electrode. The kinetic study proved that this 1D graphitic fiber has more pseudocapacitance contribution to total charge-storage than a commercial graphitic powder sample. Moreover, the less crystalline nature of the material contributed to the decreased intercalation potential (vs Na) while relating with graphite in the same electrolyte system. The GCNFs displayed a discharge capacity of 118 mAh g^{-1} in half-cell configuration. The fabricated NIC device could deliver maximum energy and power density of 55 Wh kg^{-1} and 4.52 kW kg^{-1} at ambient

temperature conditions. Moreover, the device configuration has excellent low-temperature stability with >97% capacity retention after 5000 cycles. The study ultimately realizes the possibility of considering GCNF for well-adjusted energy-power applications.

K-Ion Capacitors (KICs). Even though potassium-ion systems are expected to have electrochemical performance similar or analogous to that of sodium systems, it has been found that the former has some advantages over the latter and also the Li-ion-based energy-storage systems:⁶⁴

- The availability of potassium in the Earth's crust ($\sim 20\,000 \text{ ppm}$) is comparable to that of sodium ($23\,000 \text{ ppm}$).
- Potassium does not react with aluminum; hence Al current collectors can be used.
- K-ion systems have working potential comparable to that of Li-based systems.
- K can be ranked between Li and Na, as it combines the fast insertion property of the Li and the cost-effectiveness of Na.
- K-ions have greater mobility inside a solvent medium than Li- and Na-ions and hence higher ionic conductivity.

Thus, KICs present the qualities of ample potassium resources, lower standard electrode potential, and low price; hence, they can be a potential replacement for LICs and NICs. However, they still face glitches like inadequate reaction kinetics, low energy density, and short lifetime, mainly due to the sizable K^+ -

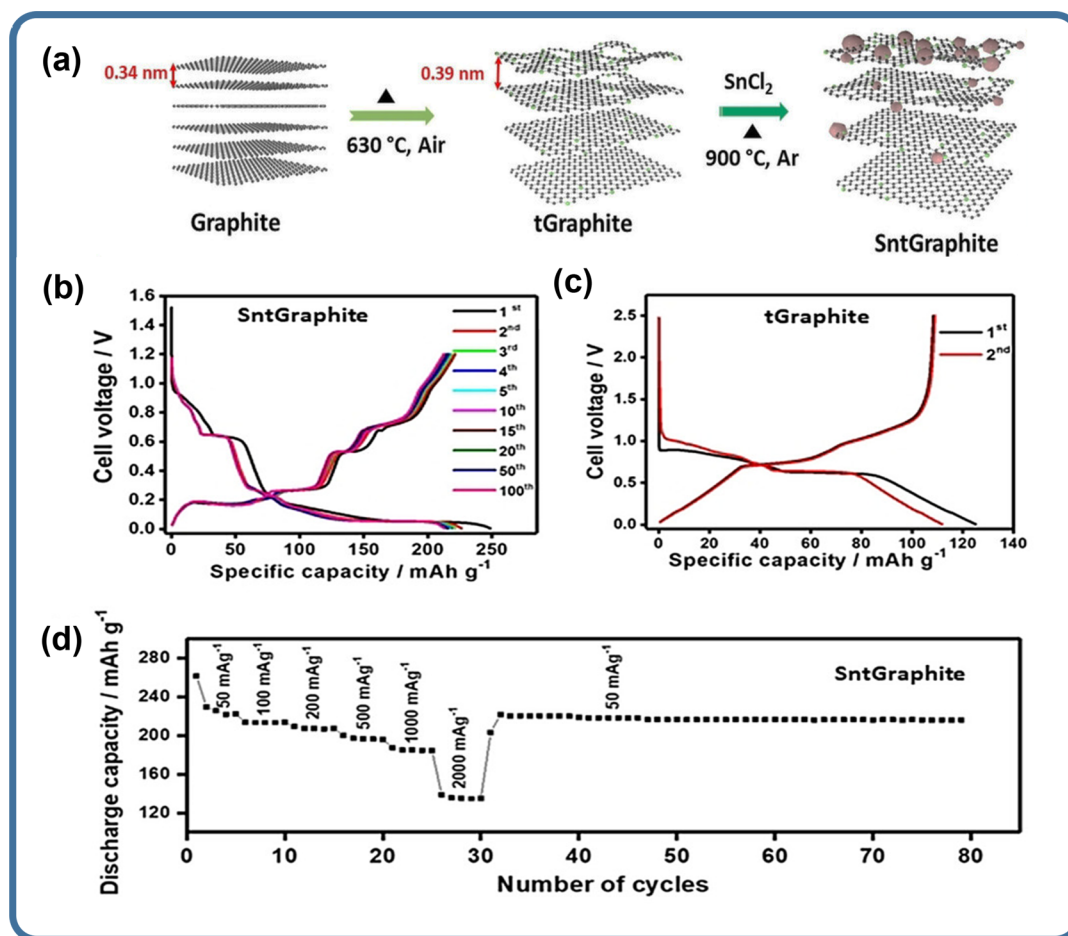


Figure 5. Snt-graphite//AC NIC: (a) synthesis pathway for Snt-graphite material, charge–discharge curves of (b) Snt-graphite and (c) t-graphite at 0.05 A g^{-1} , and (d) rate performance of Snt-graphite electrode. Reprinted with permission from ref 72. Copyright 2021 The Authors under a Creative Commons Attribution 4.0 International License, published by John Wiley and Sons.

Table 3. Electrochemical Performance of Reported Co-intercalation-Based Metal-Ion Capacitors

MIC negative// positive electrode	electrolyte	performance of MIC				
		mass ratio negative: positive	potential window (V)	maximum energy density (Wh kg^{-1})	maximum power density (kW kg^{-1})	capacity retention and cyclic stability
RG//AC LIC ⁵⁸	1 M LiPF ₆ in G ₄	1:1.5	1.3–3.8	46.40	5.6	50% after 1000 cycles at 0.5 A g^{-1}
graphitic MCMB// AC NIC ⁷⁰	1 M NaPF ₆ in G ₂	1:1.12	1–4	93.5	2.8	98.3% after 3000 cycles at 1 A g^{-1}
graphite//AC NIC ⁶⁰	1 M NaPF ₆ in G ₂	1:2.8	0–3.9	60.5	17.12	88% after 5000 cycles at $15 \text{ A g}^{-1}_{\text{graphite}}$
RG//AC NIC ⁵⁹	0.5 M NaPF ₆ in G ₄	1:1.6	1–3.75	59.93	6.84	98% after 5000 cycles at 0.5 A g^{-1}
EEG//AC NIC ⁷¹	1 M NaPF ₆ in G ₂	1:1.85	1–4.3	90	17.59	100% after 700 cycles at 0.5 A g^{-1}
GCNF//AC NIC	0.5 M NaPF ₆ in G ₂	1:1.5–2	1–3.7	55.58	4.52	80% after 3100 cycles at 1 A g^{-1}
Snt-graphite//AC NIC ⁷²	1 M NaPF ₆ in G ₂	1:1	0.005–4	93	7.8	80% after 8000 cycles at 1 A g^{-1}
graphite//AC KIC ⁶⁰	1 M KPF ₆ in G ₂	1:2.8	0–4.1	57.8	15.8	91% after 5000 cycles at $15 \text{ A g}^{-1}_{\text{graphite}}$

ion.⁷⁴ By using graphite as an anode active material, in 2017, Le Comte et al.⁷⁵ first reported the assembly of KIC. Compared with LIC technology, a significant cost reduction could be achieved in the KIC system due to the replacement of strategic materials such as Li and Cu. Liu et al.^{60,66} demonstrated the first co-intercalation-based KIC using a graphite anode, an AC cathode, and 1 M KPF₆ in G₂

electrolyte (Figure 3). Although K⁺ ions have a large ionic radius, the solvated-ion intercalation of G₂-solvated K⁺ in micro-sized graphite exhibited highly reversible and fast kinetics. The fabricated KIC delivered a capacity of $41 \text{ mAh g}^{-1}_{\text{graphite}}$ at a high specific current of $35 \text{ A g}^{-1}_{\text{graphite}}$. The device showed good cyclic stability, with more than 88% capacity retention after 5000 charge–discharge cycles and a high power

density of 15.88 kW kg⁻¹. Moreover, the KIC fabricated without pre-potassiation exhibited a high initial Coulombic efficiency and can be used for practical applications. Besides, the use of an Al current collector on both electrodes gives the assurance of a low-cost energy-storage device that can be used when the quantity of energy stored is not a vital factor while power density, cyclability, and cost are decisive. Table 3 provides a summary of the electrochemical performances of reported co-intercalation-based MICs.

■ BENEFITS AND CHALLENGES OF CO-INTERCALATION-BASED MICs

Unsettled Issues in Dual-Carbon MICs with Organic Ester-Based Electrolytes. Implementing an effective MIC is challenging as it requires a combination of capacitive and Faradaic electrodes capable of providing high energy, high power, and cyclic stability in the device configuration. Before the MIC assembly, the kinetic and capacity mismatches between EDLC-based positive and battery-type negative electrodes must be considered. Dual carbon-based MICs (DC-MICs), in which both the electrode materials are carbonaceous, hold promise for future energy-storage sector uses, mainly due to their inexpensiveness, better long-term cyclability, and improved safety. DC-LICs with an AC positive electrode and a pre-lithiated graphite negative electrode in the presence of ester-based carbonate electrolytes have been commercialized successfully. Considering the richness of Na and K compared with Li, the research also focuses on making NICs and KICs as potential alternatives to LICs.

Similar to batteries, poor coulombic efficiency, mainly due to the formation of a SEI layer on the negative electrode and a cathode–electrolyte interface (CEI) on the positive electrode, and metal plating remain as unanswered issues in the case of MICs with organic carbonate-based electrolytes.¹² Compared with commercial batteries (e.g., LIBs), SEI formation is more significant in DC-MICs. They have a reduced metal reservoir, need to lessen IR losses due to high power, and also experience more cycling. Moreover, the complete EDLC charge-storage mechanism is not precisely known for the positive electrode of MIC. CEI, a parasite oxidation product, is likely to form on the carbon electrode surface, which can be observed in first cycle capacity loss. But EDLC has a contribution even after the buildup of the CEI layer on the carbon electrode. Nanostructuring anode material also enhances electrolyte decomposition, and hence, SEI layer formation causes a low value of ICE, which has to be balanced with the pre-metal addition of negative electrodes, which is challenging to implement in practical applications.⁶⁰ Moreover, the best way to avoid metal plating issues in carbon-based LICs is to ensure that the negative electrode remains far from 0 V vs Li, mainly at intermediate and high current rates. This can be guaranteed only with the quantification using one or two reference electrodes, which is rarely done. Factors like Li scarcity, difficulties in predicting Li prices, and the requirement for a costly Cu current collector led researchers to assemble NICs and KICs to balance the future energy-storage requirements. At the same time, the large ionic radii of Na⁺ (1.02 Å) and K⁺ (1.38 Å), along with slow kinetics of battery-type negative electrodes, restrict the electrochemical performance of NICs and KICs.

How Co-intercalation-Based MICs Are Better. Co-intercalation-based MICs are assembled with graphitic carbon as battery-type negative electrode and AC as EDLC-type

positive electrode in the presence of organic ether-based electrolytes. Ethers are alleged to be less useful in Li-based systems due to poor passivation on the electrode and instability at higher voltages. Later, with the invention of co-intercalation in Na-based systems, it was revealed that ether-based electrolytes are more resistant to reduction. Hence, it leads to a thinner SEI layer formation on the negative electrode and improved ICE compared to that with ester-based electrolytes.³⁸ Studies proved that replacing the ester-based solvent with ether/G₂-based solvent ensures a thinner and uniform SEI layer, with an improved diffusion coefficient of solvated ions, and offers a perfect interface with low energy barrier and low charge-transfer resistance. Further, it was also proved that co-intercalation could enhance the rate performance and increase the pseudocapacitive contribution in the total charge-storage mechanism. Thus, the co-intercalation-based electrodes can provide fast charge-storage and long-term stability compared to conventional intercalation-based systems. In addition, graphite could be effectively used as a negative electrode material for Na- and K-based charge-storage devices.³⁰

Replacing ester-based electrolyte with ether/diglyme-based electrolyte ensures a thinner and uniform SEI layer, with an improved diffusion coefficient of solvated ions, and offers an ideal interface with low energy barrier and low charge-transfer resistance.

MICs with co-intercalation-based negative electrodes could effectively reduce the issues related to kinetic and capacity imbalance due to fast charge–discharge and lower battery-type electrode capacity, matching with that of capacitive AC electrodes. This guarantees a better electrochemical performance with high power capability and long-term stability in the assembled MIC devices. The mass ratio between positive and negative electrodes could be effectively balanced due to the low capacity of co-intercalation-based negative electrodes, which almost matched with that of AC electrodes. Thus, fabricated Na- and K-based MICs could exhibit superior electrochemical performance with high power and moderate energy, short charge–discharge time, and long-term stability compared to MICs having ester-based electrolytes. Moreover, due to high ICE values, pre-metal addition can be avoided in such MICs. These MICs also showed excellent stability at low- and high-temperature conditions. Unlike the co-intercalation-based batteries, where the unsuitability of electrolytes for the cathode can affect the full cell performance, MIC performance is not affected by the EDLC-type cathode. Figure 6 compares the performance of such MICs with the co-intercalation-based anode in the form of a Ragone plot.

Downsides of Co-intercalation-Based MICs. The main drawback of co-intercalation-based MICs are the low energy density values due to low capacity and increased operation potential of co-intercalation-based negative electrodes. The high co-intercalation potential can also reduce the voltage window of the assembled MIC device. In addition, the involvement of electrolytes in the electrode reaction creates a necessity for extra electrolytes in the cell assembly. Hence, the practical energy density of the device as a whole would get

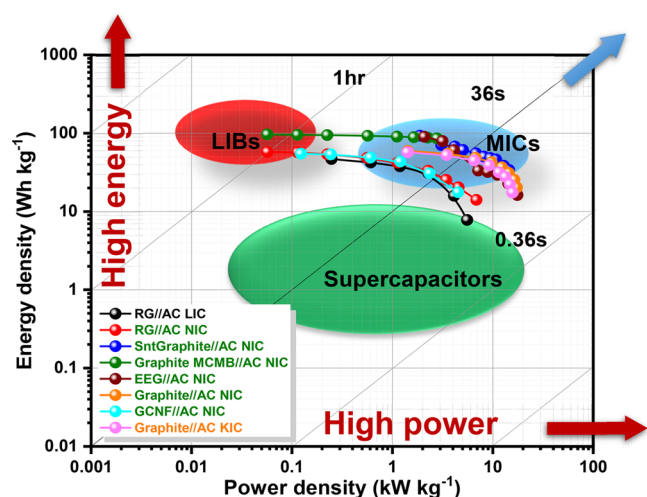


Figure 6. Ragone plot showing the position of reported co-intercalation-based MICs relative to other energy-storage technologies. The energy and power density values are calculated based on the total mass of active material present in positive and negative electrodes.

decreased. Besides, the poor understanding of reaction mechanisms such as phase formation and reaction kinetics remains a challenge.

This review focused on MICs with solvent co-intercalation and the comparison of their performance with that of conventional intercalation-based MICs (summarized in Table 2). From the reported studies, we can understand that such a prototype with an ether-based electrolyte could offer high power, fast charge–discharge, and long-term stability but less energy density compared with the ester electrolyte-based MICs. Notably, some fundamental and technical challenges exist for the future development of co-intercalation graphite electrodes in Li, Na, and K-based MICs.

1. *The dearth of knowledge on the co-intercalation mechanism.* Many issues related to the staging mechanism, phase change, and kinetics of the solvated-ion-intercalation reaction remain unclear. Solvated Na-ion intercalation into graphitic carbon material was reported as a staging mechanism. In contrast, the phase transition from stage-3 GIC to stage-2 GIC was not described by the classic staging and Dumas–Herold’s models.
2. *Nature of the SEI layer.* Regarding the nature of the SEI layer, conflicting statements still exist: (i) A SEI layer formed during the initial discharge cycle and then broke due to significant volume change originating from solvent co-intercalation and growing all through the cycles. (ii) The SEI layer formation is constrained to the first cycle and no side reactions during the subsequent cycles. This SEI layer-free nature of the reaction is assumed to be the reason behind the fast kinetics of the co-intercalation mechanism. It is also believed that the thin and robust SEI formed during the co-intercalation reaction offers cyclic stability and high coulombic efficiency for co-intercalation-based systems. Hence, there is an urgent need for further research to clarify these uncertainties.
3. *Investigation of a suitable electrode and electrolyte for co-intercalation-based negative electrode.* The compatibility of electrolytes with electrode material demands more

attention, as it can affect the electrochemical properties of the cells. Graphite works well with ether-based electrolytes but fails to perform in the case of ester-based electrolytes, mainly in the cases of Na-based systems. Besides graphite, 1D graphitic carbon nanofiber (GCNF) was also studied as a co-intercalation-based battery-type negative electrode in MICs in recent work by our group.⁷³ Co-intercalation happens specifically in the presence of glyme-based solvents (linear ethers). Moreover, the co-intercalation reduction potential changes with the length of glyme. Hence, further studies are necessary to elucidate the solvent dependence of the co-intercalation phenomenon. Besides, it is also essential to consider physicochemical properties such as viscosity, conductivity, solubility of the salt in the electrolyte, and electrochemical stability, as well as the safety and manufacturing cost of the electrolyte system, along with its feasibility for use with the electrode material.

4. *Finding the cause of chemical incompatibility of Li metal with glyme-based solvents.* Even though the assembled co-intercalation-based LIC could overshadow conventional intercalation-based LICs in terms of cyclability and safety, the half-cell performance of the co-intercalation-based negative graphitic electrode and the AC positive electrode exhibited less stability. Hence, the reasons behind the chemical instability of Li metal in ether-based electrolyte systems have to be investigated further.

The main setback of co-intercalation-based metal-ion capacitors is low energy originated from less capacity and elevated intercalation potential in negative electrodes.

5. *Methods to alleviate the volume expansion issues in graphitic materials during co-intercalation.* Co-intercalation in graphite usually incorporates a significant volume expansion during discharge. Different strategies suggested by researchers include (i) modifying the morphology of graphite anode, (ii) restricting the co-intercalation capacity, (iii) finding novel electrolytes, or (iv) designing new cell designs that can balance the volume expansion. Lessening the swelling of graphite electrodes without compromising the discharge capacity, cycle life, and power density remains an arduous task.
6. *Methods to provide flooded/extra electrolytes in the cell configuration.* One of the issues of the co-intercalation reaction is the involvement of solvent in the electrode reaction. Consuming electrolyte solvent during charging and discharging may trigger concentration fluctuations at the electrode–electrolyte interface. Hence, it is necessary to provide extra electrolytes in co-intercalation-based systems.
7. *Improving specific capacity and lowering the redox potential of co-intercalation in graphitic material.* Solvated-ion intercalation into graphite has a lower specific capacity and higher redox potential than bare-ion intercalation (except for Na-ion). It ultimately results in inadequate energy density and a reduced voltage window for the assembled MIC device. At the same time, it works

synergistically with alloying metals to enhance capacity. Decreasing the co-intercalation potential and increasing the specific capacity to obtain a high-energy, high-voltage MIC is an important topic for future studies.

8. *Improving the energy density of MIC devices.* High-capacity electrodes and a wide potential window can be employed to accomplish high energy density in MIC configuration. The limited metal-ion-storage capacity of the graphitic electrode and EDLC charge-storage of the positive carbon-based electrode has to be improved to get higher device configuration capacity. Reducing the co-intercalation reduction potential is another viable option.

Considering the viewpoints mentioned earlier, we anticipate that co-intercalation-based MICs can overcome the technical limitations, mainly in the case of energy density. They can be observed as suitable energy-storage systems where the device's high power and cycle life are crucial. Further efforts are desperately required to realize the commercialization of this fascinating mechanism in metal-ion capacitors with much more safety features.

■ ASSOCIATED CONTENT

Supporting Information

The Supporting Information is available free of charge at <https://pubs.acs.org/doi/10.1021/acseenergylett.1c01801>.

Table listing the physiochemical and thermodynamic properties of the most studied co-intercalation solvents (PDF)

■ AUTHOR INFORMATION

Corresponding Author

Vanchiappan Aravindan – Department of Chemistry, Indian Institute of Science Education and Research (IISER), Tirupati 517507, India; orcid.org/0000-0003-1357-7717; Email: aravind_van@yahoo.com

Authors

Madhusoodhanan Lathika Divya – Department of Chemistry, Indian Institute of Science Education and Research (IISER), Tirupati 517507, India

Yun-Sung Lee – School of Chemical Engineering, Chonnam National University, Gwang-ju 61186, Republic of Korea; orcid.org/0000-0002-6676-2871

Complete contact information is available at: <https://pubs.acs.org/doi/10.1021/acseenergylett.1c01801>

Notes

The authors declare no competing financial interest.

Biographies

Madhusoodhanan Lathika Divya is currently working as a Women Scientist (WOS-B) in the laboratory of Dr. V. Aravindan at IISER, Tirupati, India. Her research interest mainly focuses on transforming waste materials into electrode materials for use in charge-storage devices and hybrid ion capacitors.

Yun-Sung Lee is currently working as a Full Professor at Chonnam National University in Korea. He received his Ph.D. in 2001 from Saga University in Japan under the direction of Prof. Masaki Yoshio. His research interests lie in the fields of Li-ion batteries, electrode materials, and hybrid capacitor systems. <http://leeys.jnu.ac.kr/eng/pro/pro.php>

Vanchiappan Aravindan is currently working as an Assistant Professor at the Department of Chemistry, IISER, Tirupati, India. His research interest includes the development of high-performance electrodes and electrolytes for Li-ion batteries and beyond, including spent Li-ion battery recycling. <https://aravindvan2.wixsite.com/aravindlab>

■ ACKNOWLEDGMENTS

M.L.D. wishes to acknowledge the funding through Women Scientist Scheme-B (DST/WOS-B/2018/2039) from the KIRAN division of the Department of Science & Technology (DST), Govt. of India. V.A. acknowledges financial support from the DST through the Swarnajayanti Fellowship (DST/SJF/PSA-02/2019-20). Y.S.L. acknowledges the financial support from the National Research Foundation of Korea (NRF) grant funded by the Korean government (Ministry of Science, ICT & Future Planning) (No. 2019R1A4A2001527).

■ REFERENCES

- (1) Jiang, P.; Fan, Y. V.; Klemes, J. J. Impacts of COVID-19 on energy demand and consumption: Challenges, lessons and emerging opportunities. *Appl. Energy* **2021**, *285*, 116441.
- (2) Bertram, C.; Luderer, G.; Creutzig, F.; Bauer, N.; Ueckerdt, F.; Malik, A.; Edenhofer, O. COVID-19-induced low power demand and market forces starkly reduce CO₂ emissions. *Nat. Clim. Change* **2021**, *11* (3), 193–196.
- (3) Navon, A.; Machlev, R.; Carmon, D.; Onile, A. E.; Belikov, J.; Levron, Y. Effects of the COVID-19 Pandemic on Energy Systems and Electric Power Grids—A Review of the Challenges Ahead. *Energies* **2021**, *14* (4), 1056.
- (4) Cheshmehzangi, A. COVID-19 and household energy implications: what are the main impacts on energy use? *Heliyon* **2020**, *6* (10), No. e05202.
- (5) Kumar, J. C. R.; Majid, M. A. Renewable energy for sustainable development in India: current status, future prospects, challenges, employment, and investment opportunities. *Energy, Sustainability and Society* **2020**, *10* (1), 2.
- (6) Lukatskaya, M. R.; Dunn, B.; Gogotsi, Y. Multidimensional materials and device architectures for future hybrid energy storage. *Nat. Commun.* **2016**, *7* (1), 12647.
- (7) Gür, T. M. Review of electrical energy storage technologies, materials and systems: challenges and prospects for large-scale grid storage. *Energy Environ. Sci.* **2018**, *11* (10), 2696–2767.
- (8) Simon, P.; Gogotsi, Y.; Dunn, B. Where Do Batteries End and Supercapacitors Begin? *Science* **2014**, *343* (6176), 1210–1211.
- (9) Han, P.; Xu, G.; Han, X.; Zhao, J.; Zhou, X.; Cui, G. Lithium Ion Capacitors in Organic Electrolyte System: Scientific Problems, Material Development, and Key Technologies. *Adv. Energy Mater.* **2018**, *8* (26), 1801243.
- (10) Soltani, M.; Beheshti, S. H. A comprehensive review of lithium ion capacitor: development, modelling, thermal management and applications. *Journal of Energy Storage* **2021**, *34*, 102019.
- (11) Lamb, J. J.; Burheim, O. S. Lithium-Ion Capacitors: A Review of Design and Active Materials. *Energies* **2021**, *14* (4), 979.
- (12) Ding, J.; Hu, W.; Paek, E.; Mitlin, D. Review of Hybrid Ion Capacitors: From Aqueous to Lithium to Sodium. *Chem. Rev.* **2018**, *118* (14), 6457–6498.
- (13) Divya, M. L.; Aravindan, V. Electrochemically Generated γ -Li₂V₂O₅ as Insertion Host for High-Energy Li-Ion Capacitors. *Chem. - Asian J.* **2019**, *14* (24), 4665–4672.
- (14) Amatucci, G. G.; Badway, F.; Du Pasquier, A.; Zheng, T. An Asymmetric Hybrid Nonaqueous Energy Storage Cell. *J. Electrochem. Soc.* **2001**, *148* (8), A930.
- (15) Li, G.; Yang, Z.; Yin, Z.; Guo, H.; Wang, Z.; Yan, G.; Liu, Y.; Li, L.; Wang, J. Non-aqueous dual-carbon lithium-ion capacitors: a review. *J. Mater. Chem. A* **2019**, *7* (26), 15541–15563.

- (16) Divya, M. L.; Natarajan, S.; Lee, Y.-S.; Aravindan, V. Achieving high-energy dual carbon Li-ion capacitors with unique low- and high-temperature performance from spent Li-ion batteries. *J. Mater. Chem. A* **2020**, *8* (9), 4950–4959.
- (17) Divya, M. L.; Natarajan, S.; Lee, Y.-S.; Aravindan, V. Biomass-Derived Carbon: A Value-Added Journey Towards Constructing High-Energy Supercapacitors in an Asymmetric Fashion. *ChemSusChem* **2019**, *12* (19), 4353–4382.
- (18) Panja, T.; Ajuria, J.; Díez, N.; Bhattacharjya, D.; Goikolea, E.; Carriazo, D. Fabrication of high-performance dual carbon Li-ion hybrid capacitor: mass balancing approach to improve the energy-power density and cycle life. *Sci. Rep.* **2020**, *10* (1), 10842.
- (19) Tasaki, S.; Nagai, M.; Taguchi, H.; Matsui, K.; Takahata, R.; Kojima, K.; Ando, N.; Hato, Y.; Hatozaki, O. Lithium ion capacitor. U.S. Patent US7817403B22010.
- (20) Chen, Z.; Augustyn, V.; Jia, X.; Xiao, Q.; Dunn, B.; Lu, Y. High-performance sodium-ion pseudocapacitors based on hierarchically porous nanowire composites. *ACS Nano* **2012**, *6* (5), 4319–27.
- (21) Zhang, Y.; Jiang, J.; An, Y.; Wu, L.; Dou, H.; Zhang, J.; Zhang, Y.; Wu, S.; Dong, M.; Zhang, X.; Guo, Z. Sodium-ion capacitors: Materials, Mechanism, and Challenges. *ChemSusChem* **2020**, *13* (10), 2522–2539.
- (22) Yuan, J.; Hu, X.; Liu, Y.; Zhong, G.; Yu, B.; Wen, Z. Recent progress in sodium/potassium hybrid capacitors. *Chem. Commun.* **2020**, *56* (90), 13933–13949.
- (23) Li, Y.; Lu, Y.; Adelhelm, P.; Titirici, M.-M.; Hu, Y.-S. Intercalation chemistry of graphite: alkali metal ions and beyond. *Chem. Soc. Rev.* **2019**, *48* (17), 4655–4687.
- (24) Natarajan, S.; Aravindan, V. An urgent call to spent LIB recycling: Whys and wherefores for graphite recovery. *Adv. Energy Mater.* **2020**, *10* (37), 2002238.
- (25) Aravindan, V.; Lee, Y.-S. Building Next-Generation Li-ion Capacitors with High Energy: An Approach beyond Intercalation. *J. Phys. Chem. Lett.* **2018**, *9* (14), 3946–3958.
- (26) Moriwake, H.; Kuwabara, A.; Fisher, C. A. J.; Ikuhara, Y. Why is sodium-intercalated graphite unstable? *RSC Adv.* **2017**, *7* (58), 36550–36554.
- (27) Kim, H.; Hong, J.; Park, Y.-U.; Kim, J.; Hwang, I.; Kang, K. Sodium Storage Behavior in Natural Graphite using Ether-based Electrolyte Systems. *Adv. Funct. Mater.* **2015**, *25* (4), 534–541.
- (28) Kim, H.; Hong, J.; Yoon, G.; Kim, H.; Park, K.-Y.; Park, M.-S.; Yoon, W.-S.; Kang, K. Sodium intercalation chemistry in graphite. *Energy Environ. Sci.* **2015**, *8* (10), 2963–2969.
- (29) Jache, B.; Adelhelm, P. Use of graphite as a highly reversible electrode with superior cycle life for sodium-ion batteries by making use of co-intercalation phenomena. *Angew. Chem., Int. Ed.* **2014**, *53* (38), 10169–73.
- (30) Park, J.; Xu, Z.-L.; Kang, K. Solvated Ion Intercalation in Graphite: Sodium and Beyond. *Front. Chem.* **2020**, *8*, 432.
- (31) Goktas, M.; Bolli, C.; Berg, E. J.; Novák, P.; Pollok, K.; Langenhorst, F.; Roeder, M. v.; Lenchuk, O.; Mollenhauer, D.; Adelhelm, P. Graphite as Intercalation Electrode for Sodium-Ion Batteries: Electrode Dynamics and the Missing Solid Electrolyte Interphase (SEI). *Adv. Energy Mater.* **2018**, *8* (16), 1702724.
- (32) Xu, Z.-L.; Yoon, G.; Park, K.-Y.; Park, H.; Tamwattana, O.; Joo, Kim, S.; Seong, W. M.; Kang, K. Tailoring sodium intercalation in graphite for high energy and power sodium ion batteries. *Nat. Commun.* **2019**, *10* (1), 2598.
- (33) Kim, H.; Yoon, G.; Lim, K.; Kang, K. A comparative study of graphite electrodes using the co-intercalation phenomenon for rechargeable Li, Na and K batteries. *Chem. Commun.* **2016**, *52* (85), 12618–12621.
- (34) Cahen, S.; Speyer, L.; Lagrange, P.; Hérold, C. Topotactic Mechanisms Related to the Graphene Planes: Chemical Intercalation of Electron Donors into Graphite. *Eur. J. Inorg. Chem.* **2019**, *2019* (45), 4798–4806.
- (35) Massé, R. C.; Liu, C.; Li, Y.; Mai, L.; Cao, G. Energy storage through intercalation reactions: electrodes for rechargeable batteries. *National Science Review* **2017**, *4* (1), 26–53.
- (36) Yoon, G.; Kim, H.; Park, I.; Kang, K. Conditions for Reversible Na Intercalation in Graphite: Theoretical Studies on the Interplay Among Guest Ions, Solvent, and Graphite Host. *Adv. Energy Mater.* **2017**, *7* (2), 1601519.
- (37) Aurbach, D.; Granot, E. The study of electrolyte solutions based on solvents from the “glyme” family (linear polyethers) for secondary Li battery systems. *Electrochim. Acta* **1997**, *42* (4), 697–718.
- (38) Lin, Z.; Xia, Q.; Wang, W.; Li, W.; Chou, S. Recent research progresses in ether- and ester-based electrolytes for sodium-ion batteries. *InfoMat* **2019**, *1* (3), 376–389.
- (39) Tang, S.; Zhao, H. Glymes as versatile solvents for chemical reactions and processes: from the laboratory to industry. *RSC Adv.* **2014**, *4* (22), 11251–11287.
- (40) Peljo, P.; Girault, H. H. Electrochemical potential window of battery electrolytes: the HOMO–LUMO misconception. *Energy Environ. Sci.* **2018**, *11* (9), 2306–2309.
- (41) Jache, B.; Binder, J. O.; Abe, T.; Adelhelm, P. A comparative study on the impact of different glymes and their derivatives as electrolyte solvents for graphite co-intercalation electrodes in lithium-ion and sodium-ion batteries. *Phys. Chem. Chem. Phys.* **2016**, *18* (21), 14299–14316.
- (42) Ortiz Vitoriano, N.; Ruiz de Larramendi, I.; Sacci, R. L.; Lozano, I.; Bridges, C. A.; Arcelus, O.; Enterría, M.; Carrasco, J.; Rojo, T.; Veith, G. M. Goldilocks and the three glymes: How Na⁺ solvation controls Na–O₂ battery cycling. *Energy Storage Materials* **2020**, *29*, 235–245.
- (43) Li, K.; Galle Kankanamge, S. R.; Weldeghiorghis, T. K.; Jorn, R.; Kuroda, D. G.; Kumar, R. Predicting Ion Association in Sodium Electrolytes: A Transferrable Model for Investigating Glymes. *J. Phys. Chem. C* **2018**, *122* (9), 4747–4756.
- (44) Miranda-Quintana, R. A.; Smiatek, J. Calculation of donor numbers: Computational estimates for the Lewis basicity of solvents. *J. Mol. Liq.* **2021**, *322*, 114506.
- (45) Kottam, P. K. R.; Dongmo, S.; Wohlfahrt-Mehrens, M.; Marinaro, M. Effect of Salt Concentration, Solvent Donor Number and Coordination Structure on the Variation of the Li/Li⁺ Potential in Aprotic Electrolytes. *Energies* **2020**, *13* (6), 1470.
- (46) Goktas, M.; Akduman, B.; Huang, P.; Balducci, A.; Adelhelm, P. Temperature-Induced Activation of Graphite Co-intercalation Reactions for Glymes and Crown Ethers in Sodium-Ion Batteries. *J. Phys. Chem. C* **2018**, *122* (47), 26816–26824.
- (47) Jung, S. C.; Kang, Y.-J.; Han, Y.-K. Origin of excellent rate and cycle performance of Na⁺-solvent cointercalated graphite vs. poor performance of Li⁺-solvent case. *Nano Energy* **2017**, *34*, 456–462.
- (48) Seidl, L.; Bucher, N.; Chu, E.; Hartung, S.; Martens, S.; Schneider, O.; Stimming, U. Intercalation of solvated Na-ions into graphite. *Energy Environ. Sci.* **2017**, *10* (7), 1631–1642.
- (49) Ferrari, S.; Falco, M.; Muñoz-García, A. B.; Bonomo, M.; Brutti, S.; Pavone, M.; Gerbaldi, C. Solid-State Post Li Metal Ion Batteries: A Sustainable Forthcoming Reality? *Adv. Energy Mater.* **2021**, 2100785.
- (50) Abe, T.; Fukuda, H.; Iriyama, Y.; Ogumi, Z. Solvated Li-ion transfer at interface between graphite and electrolyte. *J. Electrochem. Soc.* **2004**, *151* (8), A1120.
- (51) Yamada, Y.; Usui, K.; Chiang, C. H.; Kikuchi, K.; Furukawa, K.; Yamada, A. General Observation of Lithium Intercalation into Graphite in Ethylene-Carbonate-Free Superconcentrated Electrolytes. *ACS Appl. Mater. Interfaces* **2014**, *6* (14), 10892–10899.
- (52) Kim, H.; Lim, K.; Yoon, G.; Park, J.-H.; Ku, K.; Lim, H.-D.; Sung, Y.-E.; Kang, K. Exploiting Lithium–Ether Co-Intercalation in Graphite for High-Power Lithium-Ion Batteries. *Adv. Energy Mater.* **2017**, *7* (19), 1700418.
- (53) Jache, B.; Adelhelm, P. Use of Graphite as a Highly Reversible Electrode with Superior Cycle Life for Sodium-Ion Batteries by Making Use of Co-Intercalation Phenomena. *Angew. Chem., Int. Ed.* **2014**, *53* (38), 10169–10173.
- (54) Jian, Z.; Luo, W.; Ji, X. Carbon Electrodes for K-Ion Batteries. *J. Am. Chem. Soc.* **2015**, *137* (36), 11566–11569.

- (55) Cohn, A. P.; Muralidharan, N.; Carter, R.; Share, K.; Oakes, L.; Pint, C. L. Durable potassium ion battery electrodes from high-rate cointercalation into graphitic carbons. *J. Mater. Chem. A* **2016**, *4* (39), 14954–14959.
- (56) Wang, L.; Yang, J.; Li, J.; Chen, T.; Chen, S.; Wu, Z.; Qiu, J.; Wang, B.; Gao, P.; Niu, X.; Li, H. Graphite as a potassium ion battery anode in carbonate-based electrolyte and ether-based electrolyte. *J. Power Sources* **2019**, *409*, 24–30.
- (57) Li, L.; Liu, L.; Hu, Z.; Lu, Y.; Liu, Q.; Jin, S.; Zhang, Q.; Zhao, S.; Chou, S.-L. Understanding High-Rate K⁺-Solvent Co-Intercalation in Natural Graphite for Potassium-Ion Batteries. *Angew. Chem., Int. Ed.* **2020**, *59* (31), 12917–12924.
- (58) Divya, M. L.; Lee, Y.-S.; Aravindan, V. Li-ion Capacitor via Solvent-Co-Intercalation Process from Spent Li-ion Batteries. *Batteries & Supercaps* **2021**, *4* (4), 671–679.
- (59) Divya, M. L.; Natarajan, S.; Lee, Y.-S.; Aravindan, V. Highly Reversible Na-Intercalation into Graphite Recovered from Spent Li-Ion Batteries for High-Energy Na-Ion Capacitor. *ChemSusChem* **2020**, *13* (21), 5654–5663.
- (60) Liu, X.; Elia, G. A.; Qin, B.; Zhang, H.; Ruschhaupt, P.; Fang, S.; Varzi, A.; Passerini, S. High-power Na-ion and K-ion hybrid capacitors exploiting cointercalation in graphite negative electrodes. *ACS Energy Letters* **2019**, *4* (11), 2675–2682.
- (61) Levi, M. D.; Levi, E. A.; Aurbach, D. The mechanism of lithium intercalation in graphite film electrodes in aprotic media. Part 2. Potentiostatic intermittent titration and in situ XRD studies of the solid-state ionic diffusion. *J. Electroanal. Chem.* **1997**, *421* (1), 89–97.
- (62) Liang, H.-J.; Hou, B.-H.; Li, W.-H.; Ning, Q.-L.; Yang, X.; Gu, Z.-Y.; Nie, X.-J.; Wang, G.; Wu, X.-L. Staging Na/K-ion de-/intercalation of graphite retrieved from spent Li-ion batteries: in operando X-ray diffraction studies and an advanced anode material for Na/K-ion batteries. *Energy Environ. Sci.* **2019**, *12* (12), 3575–3584.
- (63) Kondo, Y.; Fukutsuka, T.; Miyazaki, K.; Miyahara, Y.; Abe, T. Investigation of Electrochemical Sodium-Ion Intercalation Behavior into Graphite-Based Electrodes. *J. Electrochem. Soc.* **2019**, *166* (3), A5323–A5327.
- (64) Samantara, A. K.; Ratha, S., Metal-Ion Capacitors. In *Metal-Ion Hybrid Capacitors for Energy Storage: A Balancing Strategy Toward Energy-Power Density*, Samantara, A. K., Ratha, S., Eds. Springer International Publishing: Cham, 2020; pp 23–94.
- (65) Zou, K.; Cai, P.; Cao, X.; Zou, G.; Hou, H.; Ji, X. Carbon materials for high-performance lithium-ion capacitor. *Current Opinion in Electrochemistry* **2020**, *21*, 31–39.
- (66) Aravindan, V.; Ulaganathan, M.; Madhavi, S. Research progress in Na-ion capacitors. *J. Mater. Chem. A* **2016**, *4* (20), 7538–7548.
- (67) Wang, H.; Zhu, C.; Chao, D.; Yan, Q.; Fan, H. J. Nonaqueous Hybrid Lithium-Ion and Sodium-Ion Capacitors. *Adv. Mater.* **2017**, *29* (46), 1702093.
- (68) Subramanyan, K.; Divya, M. L.; Aravindan, V. Dual-carbon Na-ion capacitors: progress and future prospects. *J. Mater. Chem. A* **2021**, *9* (15), 9431–9450.
- (69) Zhu, J.; Roscow, J.; Chandrasekaran, S.; Deng, L.; Zhang, P.; He, T.; Wang, K.; Huang, L. Biomass-Derived Carbons for Sodium-Ion Batteries and Sodium-Ion Capacitors. *ChemSusChem* **2020**, *13* (6), 1275–1295.
- (70) Han, P.; Han, X.; Yao, J.; Zhang, L.; Cao, X.; Huang, C.; Cui, G. High energy density sodium-ion capacitors through co-intercalation mechanism in diglyme-based electrolyte system. *J. Power Sources* **2015**, *297*, 457–463.
- (71) Huang, T.; Liu, Z.; Yu, F.; Wang, F.; Li, D.; Fu, L.; Chen, Y.; Wang, H.; Xie, Q.; Yao, S.; Wu, Y. Boosting Capacitive Sodium-Ion Storage in Electrochemically Exfoliated Graphite for Sodium-Ion Capacitors. *ACS Appl. Mater. Interfaces* **2020**, *12* (47), 52635–52642.
- (72) Palaniselvam, T.; Babu, B.; Moon, H.; Hasa, I.; Santhosha, A. L.; Goktas, M.; Sun, Y.-N.; Zhao, L.; Han, B.-H.; Passerini, S.; Balducci, A.; Adelhelm, P. Tin-Containing Graphite for Sodium-Ion Batteries and Hybrid Capacitors. *Batteries & Supercaps* **2021**, *4* (1), 173–182.
- (73) Divya, M. L.; Jayaraman, S.; Lee, Y.-S.; Aravindan, V. High energy Na-Ion capacitor employing graphitic carbon fibers from waste rubber with diglyme-based electrolyte. *Chem. Eng. J.* **2021**, *426*, 130892.
- (74) Liu, M.; Chang, L.; Le, Z.; Jiang, J.; Li, J.; Wang, H.; Zhao, C.; Xu, T.; Nie, P.; Wang, L. Emerging Potassium-ion Hybrid Capacitors. *ChemSusChem* **2020**, *13* (22), 5837–5862.
- (75) Le Comte, A.; Reynier, Y.; Vincens, C.; Leys, C.; Azaïs, P. First prototypes of hybrid potassium-ion capacitor (KIC): An innovative, cost-effective energy storage technology for transportation applications. *J. Power Sources* **2017**, *363*, 34–43.